

CHARACTERIZATION OF ALLANTOINASE FROM *Escherichia coli*

A Thesis

by

JENNIFER ANN CUMMINGS

Submitted to the Office of Graduate Studies of
Texas A&M University
in partial fulfillment of the requirements for the degree of

MASTER OF SCIENCE

May 2005

Major Subject: Chemistry

CHARACTERIZATION OF ALLANTOINASE FROM *Escherichia coli*

A Thesis

by

JENNIFER ANN CUMMINGS

Submitted to Texas A&M University
in partial fulfillment of the requirements
for the degree of

MASTER OF SCIENCE

Approved as to style and content by:

Frank M. Raushel
(Chair of Committee)

Donald W. Pettigrew
(Member)

Paul F. Fitzpatrick
(Member)

Emile A. Schweikert
(Head of Department)

May 2005

Major Subject: Chemistry

ABSTRACT

Characterization of Allantoinase from *Escherichia coli*. (May 2005)

Jennifer Ann Cummings, B.S., Southern Oregon University

Chair of Advisory Committee: Dr. Frank M. Raushel

The purpose of this research was to characterize the *Escherichia coli*, *E. coli*, allantoinase enzyme. Allantoinase catalyses the conversion allantoin to allantoate via the hydrolysis of a cyclic amide bond and is coded for by the *allB* gene. The enzyme is a member of the amidohydrolase superfamily. Amidohydrolase superfamily enzymes have a common $(\alpha\beta)_8$ -barrel structure but catalyze the hydrolysis of many different substrates by a common mechanism. The structural characteristics and roles of divalent cations of enzymes in this superfamily will be discussed and related to previous work conducted on allantoinases. In this work, the metal dependence of allantoinase was initially studied by Mn, Co, Zn, Cd, and Ni-supplemented assays of enzyme of very low metal content. By changing the growth conditions under which the *allB* was overexpressed in *E. coli*, and the addition of Zn, Co or Mn to the culture, enzyme with bound Zn (ZnALN), Co (CoALN) or Mn (MnALN) was produced. The pH dependence of $\log(k_{cat}/K_M)$ for allantoinase in the presence of $MnCl_2$, ZnALN and CoALN followed a bell-shaped curve, indicating that one ionizable group needed to be deprotonated and the deprotonation of a second group caused a decrease in catalytic activity. The pK_1 for ionization at low pH was dependent upon which divalent cation was present and is

concluded to be that of the deprotonation of water. A structural model of allantoinase with bound allantoin was constructed and used to determine which amino acid residues may be involved in catalysis. Allantoinase mutants R67K, C152A, C152S, C287A, C287S, S317A, D315N and W332F were purified. The kinetic parameters k_{cat} , K_M and k_{cat}/K_M of wild type and mutant allantoinases were compared. The possible roles of these amino acid residues in catalysis and substrate binding, and the results of the pH rate profiles are discussed. A catalytic mechanism for allantoinase is proposed.

TABLE OF CONTENTS

	Page
ABSTRACT.....	iii
TABLE OF CONTENTS.....	v
LIST OF FIGURES.....	vii
LIST OF SCHEMES.....	viii
LIST OF TABLES.....	ix
LIST OF ABBREVIATIONS.....	x
INTRODUCTION.....	1
MATERIALS AND METODS.....	12
Materials and standard protocols.....	12
Cloning of the <i>allB</i> gene from <i>E. coli</i>	16
Overexpression of <i>allB</i> in pBS+.....	17
Overexpression of <i>allB</i> in pET30a+.....	17
Purification.....	18
Effects of divalent cations.....	19
Atomic absorption analysis.....	19
Enzymatic assays.....	20
Mn-cultured allantoinase growth experiments.....	20
Kinetic parameters of wild type and mutant allantoinase.....	22
pH rate profiles.....	23
Structural model of allantoinase.....	24
QuickChange mutagenesis.....	25
Creation of <i>E. coli</i> $\Delta allB$ knockout strain.....	25
Conversion of <i>E. coli</i> $\Delta allB$ to λ DE3 cells.....	29
Metal removal from ZnALN and CoALN and reconstitution.....	31
RESULTS.....	33
Cloning and overexpression of <i>allB</i>	33
Enzyme purification.....	33
Construction of <i>E. coli</i> $\Delta allB$ λ DE3 knockout strain.....	39
Effects of divalent cations.....	42
Determination of the amount of allantoin consumed.....	45

	Page
Mn-cultured overexpression of <i>allB</i>	45
pH rate profiles.....	48
Dipicolinate treatment of Zn and Co allantoinase.....	50
Reconstitution of apoALN.....	53
Structural model of allantoinase.....	53
Site-directed mutagenesis.....	59
Kinetic parameters for WT and mutant allantoinases.....	60
 DISCUSSION AND CONCLUSIONS.....	 63
 REFERENCES.....	 73
 VITA.....	 76

LIST OF FIGURES

FIGURE	Page
1 Binuclear active site of phosphotriesterase	4
2 Amino acid sequence alignment of eight allantoinases	6
3 Alternate substrates used with allantoinase.....	11
4 Agarose analytical gel for cloning of <i>allB</i>	34
5 SDS PAGE of <i>allB</i> overexpressed in <i>E. coli</i>	35
6 Sample purification of allantoinase represented by the S317A mutant	36
7 Agarose analytical gels for construction of <i>E. coli</i> $\Delta allB$	40
8 Allantoinase assayed in presence of Mn until the A ₃₄₀ no longer increased....	46
9 Activity progression of Mn-cultured overexpression of <i>allB</i>	47
10 pH rate profiles of Zn, Co and Mn allantoinase	49
11 Activity progression of ZnALN specific activity during metal removal	51
12 CLUSTALW amino acid sequence alignment of <i>E. coli</i> ALN and LHYD from <i>Arthobacter aurescens</i>	55
13 Amino acid sequence alignment of ALN and DHO from <i>E. coli</i>	56
14 The substrates for dihydroorotase, allantoinase and hydantoinase.....	57
15 Representations of the structural model of ALN.....	58
16 Substrate saturation plots for WT and mutant allantoinases.....	61
17 Possible interactions between allantoin and R67 of allantoinase.....	70

LIST OF SCHEMES

SCHEME	Page
1 Purine degradation pathway.....	2
2 Proposed catalytic mechanism of isoaspartyl dipeptidase.....	9
3 Reactions associated with the <i>o</i> -phenylenediamine enzymatic assay.....	21
4 Proposed mechanism of allantoinase.....	72

LIST OF TABLES

TABLE	Page
1 PCR thermocycles.....	14
2 Sequencing primers for the <i>AllBP-6</i> plasmid.....	15
3 Mutagenesis primers.....	26
4 Primers used in construction of the <i>E. coli</i> $\Delta allB$ strain.....	30
5 Purification summary of S317A allantoinase activity.....	37
6 Activity, metal content and protein yield of purified allantoinase samples.....	38
7 Expected PCR products for test PCR reactions from <i>E. coli</i> $\Delta allB$ DNA...	41
8 Specific activity (U/mg) of sample A ALN assayed with Co, Mn and Ni.....	43
9 Varying enhancement of different purified samples of ALN by Mn	44
10 Metal content of dipicolinate-treated ZnALN and CoALN	52
11 Specific activity for reconstitution of apoALN in the presence and absence of $Na_2S_2O_4$	54
12 Kinetic parameters for wild type and mutant allantoinases.....	62

LIST OF ABBREVIATIONS

Activity	allantoin degradation activity as assessed by the OPDA assay
ALN	allantoinase
<i>cat</i>	chloramphenicol resistance gene
CoALN	ALN from overexpression of <i>allB</i> in <i>E. coli</i> culture containing Co
DHO	Dihydroorotase
HEPES	N-(2-hydroxyethyl) piperazine-N'-(2-ethanesulfonic acid)
IAD	Isoaspartyl dipeptidase
LHYD	L-hydantoinase
MES	N-morpholino ethanesulfonic acid
MnALN	ALN from overexpression of <i>allB</i> in <i>E. coli</i> culture containing Mn
PCR	polymerase chain reaction
pET	pET30a+ vector
PIPES	Piperazine-N,N'-bis(2-ethanesulfonic acid)
SDS PAGE	sodium dodecylsulfate polyacrylamide gel electrophoresis
TABS	N-tris(Hydroxymethyl)methyl-4-aminobutanesulfonic acid
TAPS	N-tris[hydroxymethyl] methyl-3-aminopropane-sulfonic acid
WT	wild type
ZnALN	ALN from overexpression of <i>allB</i> in <i>E. coli</i> culture containing Zn

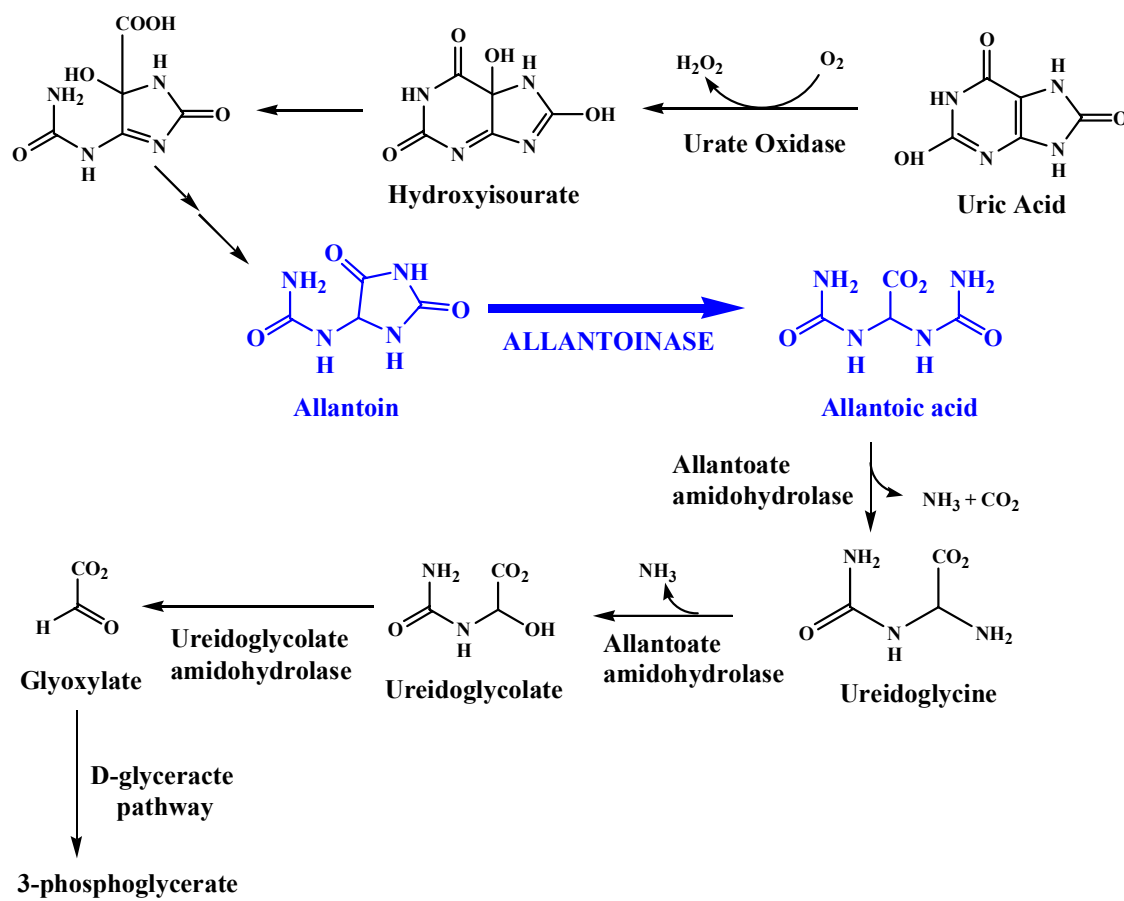
INTRODUCTION

Allantoinase catalyzes the hydrolysis of allantoin, a 5-membered heterocycle, to allantoic acid via the cleavage of a cyclic amide bond. Allantoin has skin-healing properties and is an ingredient in many topical creams. The presence of allantoin in plants is credited for the wound-healing properties of plants (1). Allantoinase (ALN) was first studied in soybeans over 70 years ago (2), but research has also been conducted on allantoinase from bacteria (3), plants (4), green algae (5), fish (2), amphibian (6) and animals (7). The enzyme is not found in humans and is part of the purine degradation pathway represented in Scheme 1 (3).

Purine degradation serves different biological roles. In plants, allantoin and allantoic acid are molecules which store nitrogen and are transported to different tissues. Allantoin and allantoic acid have high nitrogen content and little reduced carbon. When legumes are infected with nitrogen-fixing bacteria, they metabolize ureides. Purine degradation is also used to produce nitrogenous waste (4). Allantoinase plays a central role in ureide metabolism in plants because it is the last step in ureide biogenesis, and it catalyzes the first reaction of ureide degradation in tissues which store allantoin (8). The *allB* gene of *E. coli* codes for the allantoinase enzyme and is part of a regulon of genes encoding several enzymes for the degradation of allantoin to glyoxylate. Included in the regulon are genes coding for the enzymes of the D-glycerate pathway whereby glyoxylate is converted to 3-phosphoglycerate by the action of glyoxylate carboxylase,

This thesis follows the style of *Biochemistry*.

Scheme 1: Purine degradation pathway (3, 9)



tartronate semialdehyde reductase, and glycerate kinase. Under anaerobic conditions, *E. coli* can grow when allantoin is the sole nitrogen source (9). Similarly, the *B. subtilis* genome contains a cluster of genes for the conversion of hypoxanthine to uric acid and the degradation of uric acid to ureidoglycolic acid. *B. subtilis* is able to utilize uric acid, allantoin, allantoic acid, adenine, guanine, as well as the uric acid precursors hypoxanthine and xanthine as the only nitrogen source under aerobic conditions (10).

Based on protein sequence alignments, allantoinase is categorized as a member of the amidohydrolase superfamily and is expected to be a metalloenzyme. It is characteristic for the enzymes in this family to have an $(\alpha\beta)_8$ -barrel structural motif of eight alternating α -helices and β -sheets. Some of these enzymes have a mononuclear active site, as is the case with Fe^{2+} in cytosine deaminase (11), or a dinuclear site such as the two Zn^{2+} ions of dihydroorotase (12) and the two Ni^{2+} ions of urease (13). Four conserved histidine residues and an aspartic acid residue serve as ligands to the active site metal(s) and are located at the ends of the β -strands. The first two histidines are part of a conserved HXH motif on one β -strand. The third and fourth histidine ligands and aspartic acid are located at the ends of different β -strands. Some amidohydrolases with dinuclear sites (e.g. dihydroorotase and phosphotriesterase), contain a carboxylated lysine residue which acts as a bidentate ligand to bridge the two metals as is the case for the active site of PTE shown in Figure 1 (14, 15). D-aminoacylase from *A. faecalis* has a cysteine residue bridging the two metals instead of a carboxylated lysine (16). Amidohydrolases are known to use other divalent cations in lieu of their native cation(s)

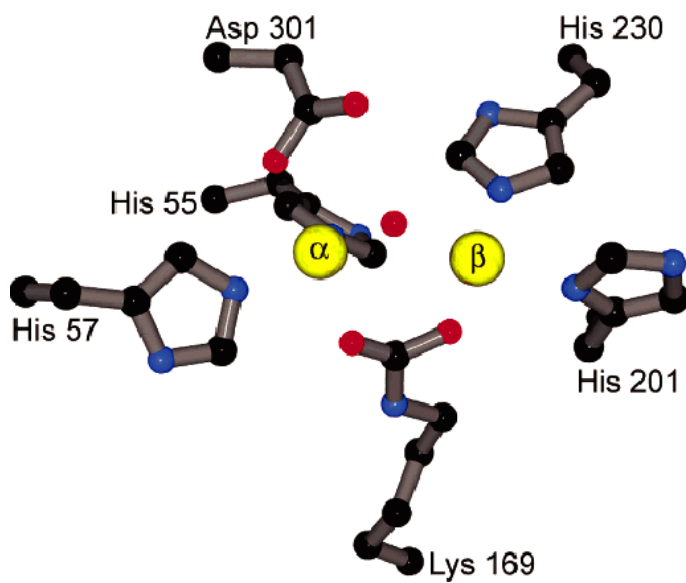


Figure 1: Binuclear active site of phosphotriesterase. Nitrogen, carbon, oxygen and Zn are colored in blue, black, red and yellow, respectively (14, 15).

such as Zn, Fe, Mn, Co, Cd, and Ni for catalytic activity (17, 18, 19). The metal ion(s) serve to activate water and polarize the substrate.

Figure 2 shows an amino acid sequence alignment of *E. coli* allantoinase with other allantoinases from bacteria, yeast and animals. Clearly, there is the conserved HXH motif, common to amidohydrolase family enzymes, and other conserved histidine, aspartic acid and lysine residues. Based on the amino acid sequence alignments of allantoinases and the *E. coli* allantoinase with the *A. aurescens* L-hydantoinase, the metal ligands are predicted to be H59, H61, H186, H242, K146 and D315. The metal ion dependence of allantoinase has been studied recently in terms of divalent cation-supplemented assays and for enzyme produced in *E. coli* cultured in media supplemented with the desired cation (20, 3). In the former case, it was found that Mn, Co, and Ni resulted in enhanced activity over enzyme assayed without divalent cation. The greatest enhancement was seen with Mn (20). By adding 2.5 mM Zn acetate, 1 mM CoCl₂, or 1 mM NiCl₂ to the *E. coli* growth media during overexpression of *allB*, Hausinger and coworkers were able to purify allantoinase with 1.4, 1.0 or 0.13 equivalents of Zn, Co, or Ni, respectively. The presence of other divalent cations such as Mn or Cd did not result in enzyme with activity higher than the control, where enzyme was produced in media without additional divalent cation salt. Incidentally, this is the only account in the literature where the metal content of allantoinase has been determined. The cobalt allantoinase contained a pentacoordinate cobalt as determined by the UV/visible absorbance of the enzyme (3). This is consistent with PTE where the

```

E. coli      -----MSFDLIIKNGTVILENEARVVDIAVKG
Yeast      -----MPINA-----ITSDHVIINGANKPATIVYSTESGTL
R. catesbeiana -----MALKSKPGIMNIIPGSKLSV-----IRSKRVIQANTISSDIIISD--GKIS
Salmonella  -----MSFDLIIKNGTVILENEARVIDIAVQG
C. felis    -----MKSSTCIFLLVIMLNCKNLVNAACTNNAAPPKI-----FRSRRVLLGDGTERDAGIVVDSSGRIK
R. pseudoacacia MDQLVWRVLPMLALLVSFLVFFYLQDSYKAQLSPFKLPGDECSLLPHRHWIWSKRIVTQQGIIISGVEINE--GEIV
B. subtilus  -----MAYDMVIKGAKAVTPDGVIEADIVVQN
B. halodurans -----MKRFDLIIRSSTVVTETTTYPRLADVAIRN

E. coli      GKIAAIG--QDLG-DAKEVMDASGLV--VSPGMVDAITVISEEPRSHWEGYETGTTRAAAKGGITMTIEMPLNQLPATV
Yeast      DVLEGSVMEKTEITKYEIHTLENVSPCTILPGLVDSVVLNLEPGRTSWEGFETGTQAASGGVTIVVDMPLNAIPPTT
R. catesbeiana SVLAWG---KHVTSGAKLLDVGDLV--VMAGIIDPVMVNEPGRTDWEGYRATLAAAAGGITAVIADMPLNSLPPTT
Salmonella  GKIAAIG--ENLG-EAKNVLDAATGLI---VSPGMVDAITVISEEPRSHWEGYETGTTRAAAKGGITMTIEMPLNQLPATV
C. felis    SIISGEEVERIANETKVEVLDDYQGFSS--IWPGVIDSIVVNEPGRRESWEGYTTATKAAAAGGITITIVDMPLNSIPPTT
R. pseudoacacia SIIEG--YGKQGNMQEAVIDYGEAV--VMPGLIDVIVVLEPGRTEWEGFDGTTRAAAGGGVTIVVDMPLNYPPTV
B. subtilus  GVIAEIG--SDIEASGTEIQADGKY---VFPGVIDCVVVFNEPGRREDWEGFETGSQMMAAGGCITYPDMLNCPSTV
B. halodurans  GIVSAITEPGSISDDGPAIDGTGLH---LFPGMVDVIVVVFNEPGRTEWEGFASGSKSLAAGGVTYFDMPLNSIPPTI
      * * * * *
      * * * * *
      * * * * *

E. coli      DRASIELKFDAAKGLTIIDAAQLGLVSY--NIDRLHELDEVGVVFVATCGDRGIDNDFRDVNDWQFFKGAQKL
Yeast      NVENFRIKLEAAEQMWCDVGFVGGGLVPH---NLPDLIPLVKAAGVRFGLFLSDG---VEEFPPIKKEYIBEALKVL
R. catesbeiana SVTNFHTKLQAAKRQCYVDVAFWGGVVPD---NQVELIPMLQAGVAGFCFLINSG---VPEFPHVSVTDLHTAMSEL
Salmonella  DRETIELKFDAAKGLTIIDAAQLGLVSY--NLDRLHELDEVGVVFVATCGDRGIDNDFRDVNDWQFFKGAQKL
C. felis    TVENLRTKVNASCKGTHVDVAFWGGVVPD---NAHELPLINAGVRFGLFTSESG---VDEFQVTKNDLEMLAKEL
R. pseudoacacia SKETLQLKLEAAEKLVVDVGFVGGGLIPENALNTSILEGLLSAGVLGVVVFMCPSG---IDDFPMTTIDHIKEGLSVL
B. subtilus  TAEHLLAKAELGRQKSAVDVAFWGGVLPV---HIEDIRPMAEAGAIFFVAFLSKSG---TDEFRSVDEPRTLKGMAEI
B. halodurans  TREELDKRQLANEKSLVDYRFVGGGLVPG---NIDHLQDLHDGGVIFVAFMSECG---TDDQFSDHETLLKGMKKI
      * * * * *
      * * * * *
      * * * * *

E. coli      GELGQVPLVVCENALICDELGEEAKREGRVTAHDYVASRPVFTVEAIRRVLYLAKVAG-----CRLHVCIVS-SPE
Yeast      AEEDTMMMFVLELPAKHEH--QQQPEQSHREYSSFLSSRPSDFEIDAINLILECLRARG-----PVPPVHIVILA-SMK
R. catesbeiana QGTNSVLLFVLELEIAKPA--PEIGDS--TLYQTFLDSRPDDMEIAAVQLVADLCQOYK-----VRCHIVVLS-SAQ
Salmonella  GEMDQTVLVVCENALICDELGEEAKREGRVTAHDYVASRPVFTVEAIRRVLYLAKAAG-----CRLHVCIVS-SPE
C. felis    QKANSVLLYVLELPAQEN--VTSNET--EKYMTYLKTRPSPMEVNAIDMIIDLTKKYK-----VRSHIVVLS-AAG
R. pseudoacacia AKYRRPLLVVAEIQQDSKNHLELKGNDPRAYLTYLNRTRPSSWEQAAIKELVDVTKDTIIGGPLEGAHVHIVLSDSSA
B. subtilus  AAAGKILALVAESDAITSYLQMVLANKGKVDADAYAASRPBEAEVEAVYRTIQYAKVTG-----CVPHVCIVS-TAK
B. halodurans  AALGSILAVVAESNEMVNAITTIATIEEQRLTVKDYSEARPIVSELEAVERILRFAQLTC-----CPIHVCIVS-SRK
      * * * * *
      * * * * *
      * * * * *

E. coli      GVEEVTRARQEGQDVTCESCPHYFVLDTDQPEEIGTLAKCSPPIRDLENQKGMWEKLFNGEIDCLVSHSPCPPPKAG
Yeast      APLIRKARASGLPVTTETCFHYLCIAAEQIPDGYTYFKCCPPIRSESNRQGLWDALREGVIGSVVSHSPCTPELKNL
R. catesbeiana SLTIIRKAKEAGAPLTVETTHYLSLSSEHIPPGATYFKCCPPVRGHRNKEALWNALLQGHIDMVSSHSPCTPDLKLL
Salmonella  GVEEVTRARQEGQDVTCESCPHYFVLDTDQPEEIGTLAKCSPPIRDQENQKGMWEKLFNGEIDCLVSHSPCPPPKAG
C. felis    ALPQLKKARSENVPLSIEBTCHHYLTFAAEDVPDGHTEYKCAPPIREESNQEKLWQALENRDIDMVSSHSPSPAALKGL
R. pseudoacacia SLDLIKEAKSRGDSISVETCPHYLAFSSSEELPDRDTRFKCSPPIRDALNKEKLEWAEVLEGHIDLLSSHSPVPPELKLL
B. subtilus  AVRLIREAKQEGLDVSVETCPHYLFLSHDDLRSQGSVAKCAPPLRSRQSKETLLETLAGDIDMVSSHSPCRPSPKRE
B. halodurans  VLKRIKQAKGEGVNVSVETCPHYLFLSDEFEAIGYLAACAPPLERQEVEDLDWGLMAGEIDLLSSHSPSLPQMKTC
      * * * * *
      * * * * *
      * * * * *

E. coli      -N-----IMKAWGGIAGLQSCMDVMFDEAVQKRGMSLPMFGKLMATNAADI FGLQ-QKG-----RIAPGKD
Yeast      QKG--DFFDSWGGIASVGLGLPLMFT---QG-CSLVDIVTWCKNTSHQVGLSHQKG-----TIAPGYD
R. catesbeiana KEG--DYMKAWGGISSLQFGLPLFWTSARTRG-FSLTDSVQLSSNTAKLCCGLGIVKEPLKWVMMIWSGGITKFSR
Salmonella  -N-----IMQAWGGIAGLQSCMDVMFDEAVQKRGMSLPMFGKLMATNAADI FGLK-HKG-----RIAPGKD
C. felis    CNGCHPDFLKAWGGIAGMQFGLSLIRTGASKRG-FKAHDVSRMAAGPAKLTGLDGIKG-----QIKEGLD
R. pseudoacacia EEG--DFLRAWGGISSLQFGLPLFWTSYGKKHG-LTLEQLSLLSLLSKPATFAGLESKG-----AIAVGNH
B. subtilus  DN-----MFLSWGGISGGQFTLLGMLELALEH-QI PFETIAEWWSAAPAKRFGLQ-KKG-----RLEAGCD
B. halodurans  KT-----IFEVWGGIAGCQNTLAVMLTEGYHKKRMLPTQIVQLTATEPAKRFGLYPQKG-----TIQVGAE
      * * * * *
      * * * * *

E. coli      ADFVFIQP-NSSVLTNDD--LEYRHKVSPYVG--RTIGARITKTI LRGDVIYDIEQGFVPVAPKGFILKHQQ-----
Yeast      ADLVVFDT-ASKHKISNSS--VYFNKLTAYNG--MTVKGTVLKTILRGQWYIRMPTESRKHHWVKLCLILDVVKLKLQI
R. catesbeiana CKKMIFITRISSPHIWDSP--FKEKSWLLLFGLLFISKGSMLPNQLENFLYTLWLSLVKPVHPVHPHPIRKNLPHI---
Salmonella  ADLVFIQP-DSSYVLKNED--LEYRHKVSPYVG--RTIGARITKTI LRGDVIYDIEHGFVPVPKGFILKHQQ-----
C. felis    ADLVIWDP-EEEFKVTKDI--IQHKNKETPYLVG--MTLKGKVHATVVRGDFVYRN--GQPFEPKGNLLIE-----
R. pseudoacacia ADIVVWQP-ELEFDLNDYVPVFIKHPSL SAYMG--RRLSGKVLDTFVRGNLVFKD--GKHAPAACGVPI LAK-----
B. subtilus  ADFVLVSM--EPYTVTRES--MFAKHKHSIYEG--HTFPCSI SATYSKGRVYNDGKVTEDIGALVVP-----
B. halodurans  ASFTLIDL-NESYTLNASD--LYYRHPI SPYVG--QRFRGKVKHTICQGHVYQDH-----
      *

```

Figure 2: Amino acid sequence alignment of eight allantoinases. Residues are colored according to complete conservation (blue with asterisks), predicted metal ligands (green highlight), predicted β -sheet locations (magenta). Residues which may contact the substrate are highlighted in violet.

metals are pentacoordinate (15) and with IAD where a tyrosine residue is in proximity with one metal (21) as a fifth ligand.

In binuclear amidohydrolase enzymes, there is a buried α metal and a more solvent-exposed β . The specific roles of these two metal ions have been elucidated by studies with phosphotriesterase, PTE. The Zn/Cd form of PTE is a single hybrid enzyme with Zn bound in the buried α site and the Cd in the β site. Based on the crystal structure of PTE with the inhibitor diisopropyl methylphosphonate bound to the enzyme and pH rate profile comparisons of Zn/Zn, Cd/Cd and Zn/Cd PTE, it has been proposed that the α metal plays a dominant role in the pK_a of water and the β metal functions primarily to polarize the substrate (14). This is consistent with the crystal structure of dihydroorotase (DHO) with bound dihydroorotate where the β Zn metal is 2.9 Å from the carbonyl oxygen of the amide bond hydrolyzed by the enzyme (12). The crystal structure of diisoaspartyl dipeptidase (IAD) with the bound aspartate product shows how the carboxylate, formed by the cleavage of an amide bond, is positioned with respect to the two Zn ions (21).

Enzyme superfamilies are groups of enzymes which catalyze different reactions by a common reaction mechanism (22). A catalytic mechanism has been proposed for PTE, DHO and IAD where an activated water hydroxyl is the nucleophile and the aspartic acid bound to the α metal is involved in acid/base catalysis. Aspartic acid acts as a base during the nucleophilic attack on the carbonyl carbon of the amide bond in dihydroorotate or the isoaspartyl dipeptide, or on the phosphorus of the phosphate ester of paraoxon, to form a quaternary intermediate. The quaternary intermediate is

stabilized by the two metals. The aspartic acid residue then acts as an acid during bond cleavage. The proposed catalytic mechanism of IAD is shown in Scheme 2 as an example of this conserved mechanism (21).

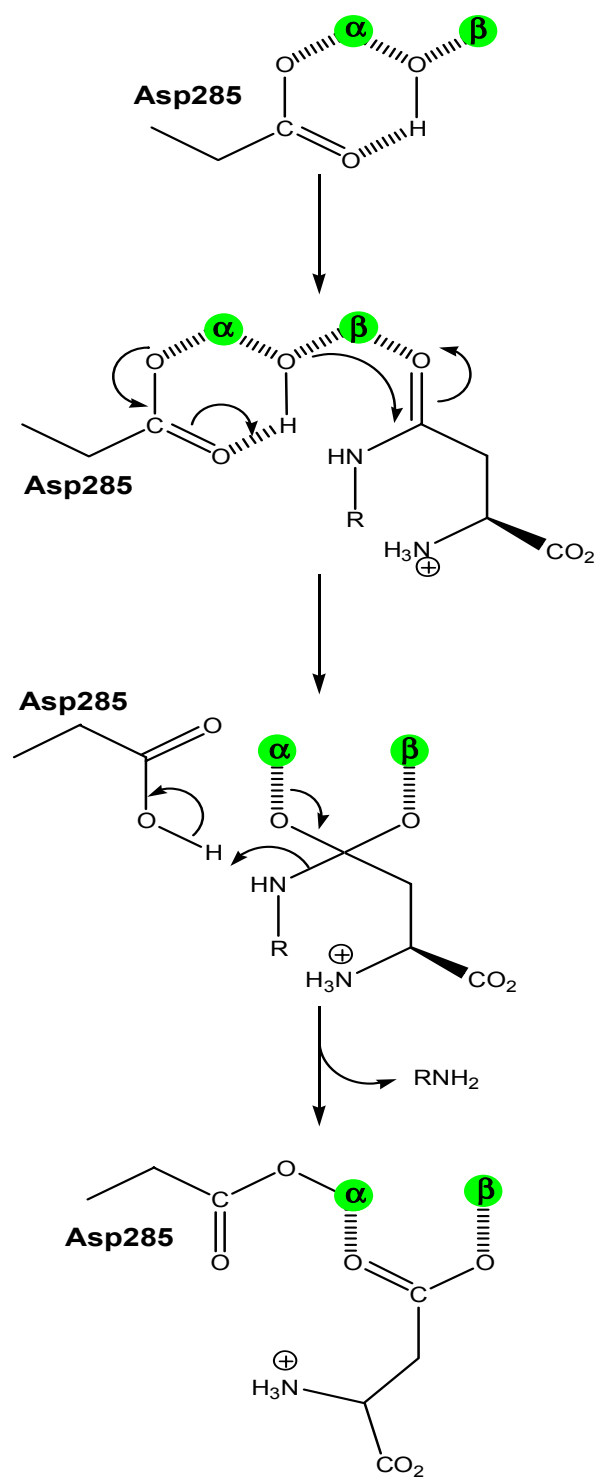
The quaternary structure of *E. coli* ALN is expected to be a homotetramer with subunits of 50 kDa in size (20). However, allantoinases have been known to exist as monomers (23), and also in a heterotetramer complex with allantoicase (24).

Allantoicase is the enzyme following allantoinase in the purine degradation pathway.

Other cyclic amidases such as dihydropyrimidinase (25), L-hydantoinase (26) and D-hydantoinase (27) also exist as homotetramers in the form of a dimer of dimers.

Amidohydrolase superfamily enzymes are also known to exist as dimers (e.g. DHO), hexamers (e.g. trimer of dimers for *E. coli* cytosine deaminase) and octamers (e.g. tetramer of dimers for IAD) with identical subunits (12, 11, 21).

Allantoinases from various bacteria, plants, and animal sources were extensively studied by Vogels and coworkers (2). The bacterial strains were chosen from bacteria which were able to grow in media where allantoin was the main source of nitrogen. It was found that allantoinases differed greatly in their properties. For example, allantoinases of *A. allantoicus*, *S. allantoicus*, and *E. coli* were considered to be activated by, and dependent upon Mn^{2+} . The pH optima ranged from 7 to 8.5. The K_M values of different species varied greatly from 5 to 46 mM. It is interesting to note that all of the bacterial allantoinases had very distinct pH optima. The activities dropped significantly above and below a narrow pH range (about 0.5 Δ pH units or less). This is in contrast to the animal and plant allantoinases which had extended pH optima. In the same study, it

Scheme 2: Proposed catalytic mechanism of isoaspartyl dipeptidase (21)

was thought that *A. allanoicus*, *S. allantoicus*, and *E. coli* allantoinases were non-specific for either (+) or (-) allantoin. Other species had a preference for (+) allantoin (2). In contrast to this, Hausinger and coworkers found that *E. coli* allantoinase selectively catalyzed the hydrolysis of S-allantoin resulting in conversion of only one half of the substrate present (3). The structures for methylolallantoin and 5-aminohydantoin are shown in Figure 3, and were used as substrates for allantoinase; the degradation rates for these compounds by allantoinase varied greatly among species (2). The position of the methylol group was unknown but thought to be on position N6 or N8 of allantoin. Other substrates, presented in Figure 2, have also been used with the *E. coli* ALN more recently but with much less activity than with allantoin as the substrate (20).

In two recent publications, the reported K_M for allantoinase from *E. coli* ALN were quite different, namely 4 mM (20) and 17 mM (3), but had similar values for pH optima. Furthermore, it has been mentioned that reducing agents stimulate bacterial ALN such as that from *E. coli*, but inhibit the activity of plant and animal ALN (1).

To date, the allantoinase crystal structure has not been solved and therefore, the structural details have not yet been elucidated. Site-directed mutagenesis has not been used to identify essential residues for catalysis or those which might interact with the substrate. Even though allantoinase has been purified with Zn, Co or Ni present, the affect of different metals on the pK_a of water has not been determined. The roles of the active site cations, likely to be binuclear Zn, have not been completely clarified.

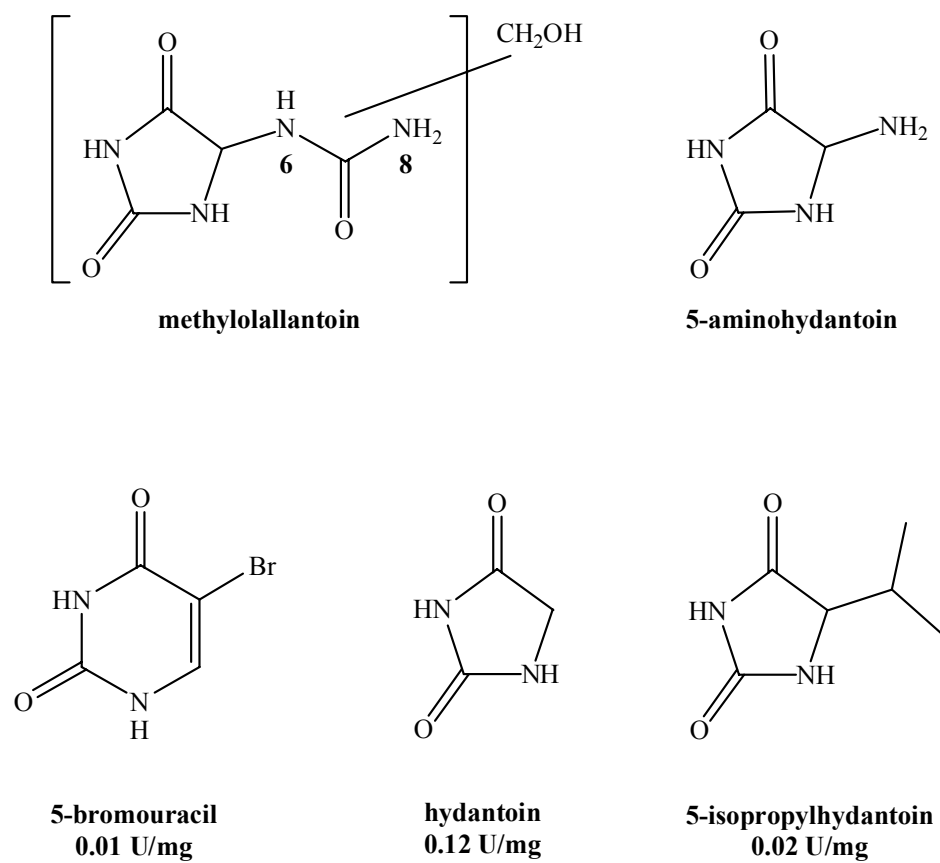


Figure 3: Alternate substrates used with allantoinase (2, 20). The specific activities shown are compared to that with allantoin of 6.6 U/mg (20).

MATERIALS AND METHODS

MATERIALS AND STANDARD PROTOCOLS

Solutions of Luria-Bertani (LB) broth consisted of tryptone, yeast extract and NaCl in concentrations of 10 g, 5 g, and 5 g per liter, respectively. Terrific broth (TB) media contained 12 g, 24 g, 5 g, 2.3 g, and 12.5 g per liter of tryptone, yeast extract, glycerol, potassium phosphate monobasic, and potassium phosphate dibasic, respectively. SOB medium contained 20 g tryptone, 5.0 g yeast extract, 0.5 g NaCl per liter as well as 10 mM each of MgSO₄ and MgCl₂. Unless otherwise specified, the concentrations of ampicillin, kanamycin and chloramphenicol used were 100 µg/ml, 50 µg/ml, and 25 µg/ml, respectively for all liquid and solid media.

E. coli cell strains were made electrocompetent by a standard protocol, unless otherwise specified. The *E. coli* cell strains XL1 Blue and BL21 λDE3 were obtained from Stratagene. Liquid LB was first inoculated with cells of interest and grown overnight at 37 °C. This culture was used to inoculate a larger culture at a ratio of 5 ml overnight culture per liter of larger culture LB. In the case of $\Delta allB$ BWcam9 knockout cells, chloramphenicol was present in all cultures. The larger culture was incubated at 37 °C until the OD₆₀₀ reached ~ 0.5. The cells were harvested and washed three times with 1X, 0.5X and 0.25X the large culture volume, consecutively, with ice cold 10% v/v sterile glycerol. Glycerol was used as a cryoprotectant (28). Cells were stored at ~ 100-fold higher cell concentration than the large growth culture in 10% glycerol. All gel purifications of DNA were performed in 1% low melting point agarose containing 0.5

g/L ethidium bromide. Standard 1% agarose was used for analytical purposes. Agarose gels were photographed under ultraviolet illumination.

Plasmid DNA (with or without *allB*) was amplified by growth of electrotransformed cells in LB/kanamycin. Plasmid DNA was purified from cells using the Wizard[®] *Plus* SV Minipreps DNA Purification System from Promega, following the protocol outlined for Gram-negative bacteria. All purified DNA was stored in nuclease-free water at -20 °C for short term storage and at -80 °C for long term storage.

All primers used in polymerase chain reactions were ordered from IDT and dissolved in nuclease-free water. In all cases, the stock of 10 mM dNTP PCR nucleotide mix from Promega was used. All PCR reactions were performed in an MJ Research PTC-200 thermocycler. Restriction enzymes were from New England Biolabs. The *Pfx* Platinum polymerase kit (amplification buffer, 50 mM MgSO₄, enhancer solution and *Pfx* Platinum polymerase) from Novagen was used to obtain PCR products for the construction of the *E. coli* $\Delta allB$ knockout strain and in the cloning of *allB* from PBS+ to pET30a+ (Novagen). *Pfu* Turbo polymerase and *DpnI* enzymes from Stratagene were used in all PCR reactions for QuickChange[®] mutagenesis. A description of all PCR temperature cycles is outlined in Table 1 and is the reference for every PCR program mentioned with its associated number. The sequencing primers used to confirm the *allB* sequence in pET are outlined in Table 2. Each sequencing reaction consisted of 1-4 μ L of DNA, 2 μ L Perkin Elmer ABI Big Dye Reaction Mix (5X Tris buffer pH 9.0, dNTP mix, ddNTPs, Amplitaq FS enzyme), 2 μ L of one 5 pmol/ μ L sequencing primer

Table 1: PCR thermocycles

PCR Program #	Step 1: DNA duplex	Step 2: DNA duplex	Step 3: Primer	Step 4: DNA extension	Repeat Steps	Step 5: Final extension
1 (<i>allB</i> clone)	95°C 30 sec	95°C 30 sec	50°C 1 min	60°C 4 min	2-4, 40 times	68°C 10 min
2 (QC mut)	95°C 30 sec	95°C 30 sec	55°C 1 min	68°C 14 min.	2-4, 17 times	---
3 (QC mut 2)	95°C 30 sec	95°C 30 sec	60°C 1 min	72°C 14 min.	2-4, 17 times	---
4 (cam9)	95°C 5 min	95°C 30 sec	50°C 1 min	60°C 4 min	2-4, 40 times	68°C 10 min
5 (Δ <i>allB</i> tests)	95°C 5 min	95°C 1 min	53°C 4 min	60°C 4 min	2-4, 40 times	68°C 10 min
6 (SQ)	95°C 30 sec	95°C 30 sec	50°C 1 min	60°C 4 min	2-4, 99 times	

Table 2: Sequencing primers for the *AllBP-6* plasmid

Primer Name	PCR primer nucleotide sequence 5 →3'
T7 promoter primer	TAATACGACTCACTATAGGG
T7 terminator primer	GCTAGTTATTGCTCAGCGG
allB-f	GTGGGCGTTGTCGGCTTC

(internal *allB* gene primer: *allB*-f, T7 promoter, T7 term) and nuclease-free water to yield a 10 μL reaction. The thermocycle used for amplification of DNA for sequencing was program # 6.

The absorbance at 280 nm was used to determine the concentration of enzyme. The extinction coefficient, $\epsilon_{280} = 35,720 \text{ cm}^{-1}\text{M}^{-1}$ (29), was calculated based on the amino acid sequence (30). For purification steps before gel filtration fractions, the enzyme concentration was determined using the Bradford assay (31) with standards of 4 to 28 $\mu\text{g}/\text{mL}$ bovine serum albumin and the Quick Start Bradford Dye Reagent from BioRad. For growth experiments, the Bradford assay was also used to determine the protein concentration of cell extracts after treatment with Bugbuster[®] protein extraction reagent (Novagen).

CLONING OF THE *allB* GENE FROM *E. coli*

PCR was used to amplify the *allB* gene from the pMU-6 clone of *allB* into pBS+. A 100 μL PCR reaction contained 1X *Pfx* amplification buffer, 1.0 mM MgSO_4 , 200 μM dNTP PCR mix, pMU-6 DNA, 3X enhancer solution, 5 units *Pfx* platinum polymerase, and 1 μM each of primers 1 (5'→3': GCCGGGCCATATGTCTTTGATTTAATCATTA A) and pBSA₂ (5'→3'CTGTTGGGAAGGGCGATC). Primers 1 and 2 incorporated *NdeI* and *EcoRI* restriction sites at the ends of the amplified gene, respectively. The thermocycle followed PCR program #1. The purified PCR product was cloned into the *EcoRI* and *NdeI* restriction sites of the pET30a+ vector via ligation with T4 ligase. Competent XL1 Blue *E. coli* cells were electrotransformed with the ligation product (40 μL cells, 5 μL ligation reaction), plated on LB/kanamycin and grown at 37 °C overnight.

Kanamycin-resistant colonies were used to inoculate LB/kanamycin and obtain multiple copies of DNA for selected clones from overnight cultures (37 °C). Clones were selected for DNA sequence determination. The clone noted as *AllBP-6* was selected for overexpression of wild type *allB* and as template DNA for QuickChange[®] mutagenesis.

OVEREXPRESSION OF *allB* IN pBS+

The pBS+ plasmid containing ampicillin resistance and *allB* genes, specifically the pMU-6 clone, was used to electrotransform competent BL21 cells. Single ampicillin resistant colonies were used to inoculate 5 ml LB overnight cultures containing 50 $\mu\text{g/ml}$ ampicillin. Each overnight culture was grown at 37 °C and used to inoculate one liter of TB media containing 50 $\mu\text{g/ml}$ of ampicillin. The TB cultures were grown at 37 °C and induced with 500 μM isopropyl β -thiogalactosidase, IPTG, when the optical density of the cultures reached an OD₆₀₀ value between 0.7 to 0.9. After the addition of IPTG, the cells were grown at 37 °C for 5.5 hours. To produce enzyme with higher content of Zn or Mn, *allB* in pBS+ was also overexpressed in TB media containing 250 μM ZnCl₂ or MnCl₂. The protocol was later changed in that 50 μM IPTG was added at OD₆₀₀ ~ 0.1-0.2. After the addition of IPTG, the cells were grown at room temperature (~22-23 °C) for 16-18 hours.

OVEREXPRESSION OF *allB* IN pET30a+

In the pET30a+ vector, *allB* was overexpressed in *E. coli* grown in TB media enriched with 2.5 mM Zn acetate, 1.0 mM CoCl₂ or 3.0 mM MnSO₄. In each case, the cells were grown at 30 °C prior to induction with 50 μM IPTG. Following the addition

of IPTG when the optical density reached an $OD_{600} \sim 0.1-0.2$, the cells were grown at room temperature ($\sim 22-23\text{ }^{\circ}\text{C}$) for 16-18 hours.

The incubation temperature after addition of IPTG was lowered to range between $13-15\text{ }^{\circ}\text{C}$. All allantoinase mutants were overexpressed under these cooler conditions as was wild type ZnALN for comparison. In order to obtain $\sim 3.4-13$ g cells per liter of culture, cells were harvested 23-39 hours after the addition of IPTG.

PURIFICATION

Allantoinase was purified from $\sim 10-16$ g cells. Using 50 mM HEPES pH 8.1, the cells were homogenized in a total volume of 6 mL/g of cells in the presence of 100 $\mu\text{g/ml}$ phenylmethylsulfonylfluoride (Sigma) and 1 $\mu\text{g/ml}$ RNase A. The homogenate was sonicated on ice for ~ 10 minutes, at 5-second on and off intervals and cooled for ~ 10 minutes. The sonication was repeated until the cells had been sonicated for 30-40 minutes. The sonicated cells were centrifuged and the pellet discarded. Twenty percent ammonium sulfate (107.5 g/L) was added to the sonication supernatant, discarding the pellet after centrifugation. Fifty percent ammonium sulfate (additional 188 g ammonium sulfate/L 20% supernatant) was then used to precipitate allantoinase. Following centrifugation, the 20-50% ammonium sulfate pellet was dissolved in a minimal amount of 50 mM HEPES, pH 8.1 and loaded in its entirety onto a ~ 3 L A34 gel filtration column. Allantoinase was eluted from the column with 50 mM HEPES, pH 8.1, at a flow rate of 1 mL/min. The A34 column has a linear separation range of 20-320 kDa. The absorbance at 280 nm of the collected fractions was plotted against fraction number to identify protein peaks to analyze by SDS/PAGE. The exception to this purification

protocol was that of CoALN. The 20-50% ammonium sulfate pellet for CoALN was loaded onto a 120 ml Superdex 200 HPLC column. Using a flow rate of 1.0 ml/min, allantoinase eluted after ~ 68-80 ml.

EFFECTS OF DIVALENT CATIONS

One sample of enzyme purified after overexpression in pBS+ was assayed with 20 mM allantoin, pH 8.0, in the presence of 25-500 μ M CoCl₂, NiCl₂, MnCl₂, ZnCl₂ and CdCl₂. Other subsequent samples were assessed for the level of activity enhancement by 25 μ M MnCl₂.

ATOMIC ABSORPTION ANALYSIS

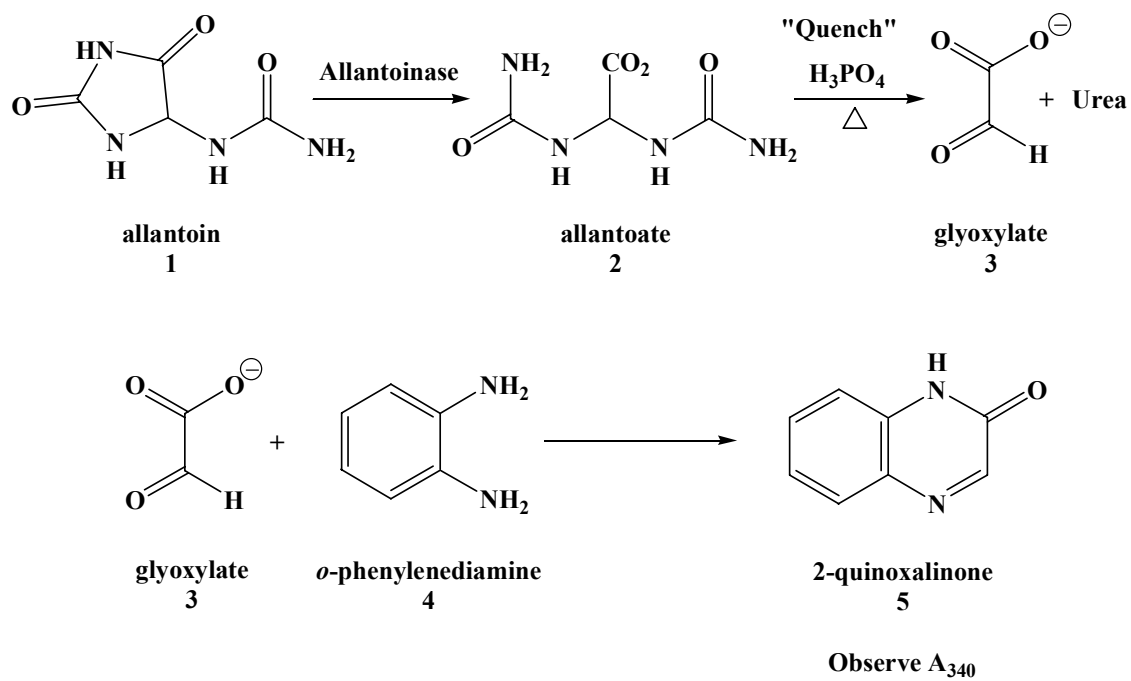
For every sample of purified enzyme, atomic absorption (AA) analysis was used to determine the Zn content of the protein and when appropriate, the Mn or Co content. Standards of Zn (1-6 μ M), Co (8.5-85 μ M), and Mn (5-80 μ M) were prepared from dilutions of a 1000 μ g/ml manufactured stocks with 0.5% v/v nitric acid. Different concentrations of enzyme were analyzed and the equivalents of metal per subunit were determined from concentration values that were within the standard range. Enzyme was diluted with metal-free buffer and analyzed by AA. For enzyme purified from overexpression in pET30, enzyme (1-2.5 mg) was eluted through an 8 ml PD-10 (Pharmacia) column to remove unbound metal and then diluted to the desired concentration with metal-free buffer (50 mM HEPES pH, 8.1). Metal-free buffer was obtained by equilibrating a slurry of BioRad Chelex 100 Resin and 50 mM HEPES pH 8.1 and subsequent collection of the buffer through a filtered column.

ENZYMATIC ASSAYS

The assay used to determine the activity of allantoinase is an indirect coupling system designed by Hausinger and coworkers (32) and is illustrated in Scheme 3. The first step of the assay is the conversion of allantoin (1) to allantoic acid (2) by allantoinase. For each 1.0 ml assay, several 80 μ L aliquots were removed over time and quenched into 320 μ L of an *o*-phenylenediamine, OPDA, solution (1.0 mg/ml *o*-phenylenediamine, 0.2% v/v β -mercaptoethanol, 1.0 M phosphoric acid, pH 2.0). Upon boiling of the quenched aliquots for 3 minutes, the allantoic acid is converted to glyoxylate (3). Glyoxylate and OPDA (4) react to form the final product quinoxalone (5), which is monitored by absorbance at 340 nm, A_{340} , with $\epsilon_{340} = 4000 \text{ cm}^{-1}\text{M}^{-1}$. Unless otherwise specified, enzyme activity was measured under the conditions of 30 mM allantoin in 50 mM HEPES, pH 8.0 and 30 °C for purification steps and growth experiments. One unit (U) of activity is defined as the conversion of one micromole of substrate per minute. Purified sample A allantoinase was assayed in the presence of 25 μ M MnCl_2 and 6 to 18 mM allantoin until the A_{340} no longer increased.

Mn-CULTURED ALLANTOINASE GROWTH EXPERIMENTS

In the first experiment, *E. coli* BL21 cells with *allB/pET30* were grown in TB at 30 °C until the OD_{600} reached 0.2. The cells were further grown at room temperature (20 °C), 30 °C or 37 °C after adding varying concentrations of IPTG (0, 50, 100, 250, 500 μ M). Over time, aliquots of cells were removed, centrifuged and frozen. Crude cell extracts of soluble protein were obtained by treatment of the cells with 1% v/v

Scheme 3: Reactions associated with the *o*-phenylenediamine enzymatic assay (32)

Bugbuster[®] protein extraction reagent (Novagen) and centrifugation. The allantoin degradation activity of crude cell extracts was assessed. Based on the results of the first experiment, a second experiment was performed in which the activity was assessed for cultures grown in the same way but under four conditions: 25 and 50 μM IPTG both with and without 3.0 mM MnSO_4 at room temperature ($\sim 19 \pm 1^\circ\text{C}$) for up to 37.5 hours. The conditions chosen for a larger scale production of MnALN were induction with 50 μM IPTG at $\text{OD}_{600} = 0.2$ followed by growth at room temperature for 37.5 hours. The enzyme was purified. For the next large scale production of MnALN, the activity of enzyme in cell extracts was monitored as the cells were grown so as to harvest the cells at the point of maximal activity. Thirty-three grams of cells were obtained from 2 L of cells grown for 18.5 hours at room temperature after addition IPTG and used to purify MnALN.

KINETIC PARAMETERS OF WILD TYPE AND MUTANT ALLANTOINASE

Wild type and mutant ZnALNs were assayed at varied concentrations of 5-70 mM allantoin in 50 mM HEPES, pH 8.0. Concentrated substrate was prepared by adding warm deionized water (37°C) to allantoin with the appropriate amount of 1.0 M HEPES. Allantoin was allowed to dissolve at pH 8.5, after which the solution was cooled to room temperature and the pH adjusted to pH 8.0. The concentrated substrate was immediately used to make assay solutions. Assays were performed at 20°C . The exception to this was for the kinetic parameters of sample A ALN with and without 25 μM MnCl_2 which was assayed at 30°C in TAPS buffer, pH 8.5. Velocity data ($\mu\text{mol/minute}$) were plotted as a function of allantoin concentration in mM and fit to

equation 1 for all samples except C287A, C287S, and S317A, for which equation 2 was used to determine k_{cat}/K_M . For equations 1 and 2, S refers to the substrate allantoin, k_{cat} to the catalytic turnover at substrate saturation, v to velocity, K_M to the Michaelis-Menten constant, and E_t is the total amount of enzyme.

$$\frac{v}{E_t} = \frac{k_{cat}[S]}{K_M + [S]} \quad 1$$

$$\frac{v}{E_t} = \frac{k_{cat}}{K_M}[S] \quad 2$$

pH RATE PROFILES

The pK_a values of ionizable groups were determined for ALN with 25 μM MnCl_2 in the assay, ZnALN, and CoALN. Prior to performing pH rate profile experiments, it had been determined that maximal enzyme activity could be achieved with only 25 μM MnCl_2 in the assay and was not further improved beyond this concentration when using 50 nM enzyme at pH 8.0. Due to the fact that the K_M value of the enzyme and the natural solubility of allantoin at pH 8.0 are approximately the same, performing a large number of assays for substrate saturation proved problematic, especially at lower pH. Therefore, experiments were designed using 7-48 mM allantoin, 300 nM enzyme, 25 μM MnCl_2 and 50 mM buffer for the determination of k_{cat}/K_M as a function of pH. The buffers used were PIPES (pH 6.65-6.95), HEPES (pH 7.1-7.85), TAPS (pH 8-8.45) and TABS (pH 8.6-9.8). Assays were performed at 30 °C, quenching assay aliquots at one minute intervals from 2-7 minutes after the addition of enzyme. The final pH was

determined after the completion of the assay by combining equal aliquots of the assay from each allantoin concentration. All individual assays were blanked by an endpoint quench of the same assay solution for each pH and allantoin concentration with water in place of enzyme. The $\log(k_{cat}/K_M)$ data were fit to equation 3, where K_1 and K_2 are the ionization constants for protonation and deprotonation at low and high pH, respectively.

$$\log\left(\frac{k_{cat}}{K_M}\right) = \frac{C}{1 + \frac{10^{pH}}{K_1} + \frac{K_2}{10^{pH}}} \quad 3$$

STRUCTURAL MODEL OF ALLANTOINASE

Using Swiss PDB Viewer, the ALN amino acid sequence was threaded onto the crystal structure of LHYD (26) to create a hypothetical three-dimensional structure of allantoinase. According to this structural overlay, allantoinase would most likely have a binuclear metal center with the following ligands: four histidine residues (H59 H61, H186, H242), an aspartic acid (D315) and a carboxylated lysine (K146). The ALN hypothetical structure and the dihydroorotase crystal structure (12) were overlaid by using the four histidine ligands as focal points. Dihydroorotate was converted to allantoin by removing the CH_2 group, converting the carboxylic acid group to $-\text{NH}[\text{CO}]\text{NH}_2$, and specifying the S-(+)-allantoin form. The $(-\text{NH}[\text{CO}] -)_2$ motif of dihydroorotate was kept in the same three-dimensional position.

QUICKCHANGE MUTAGENESIS

Point mutations within the *allB* gene were made using the method of QuickChange[®] mutagenesis. The composition of the PCR reaction for all allantoinase mutants were the same for the mutants C152A, C152S, C287A, C287S, S317A, H316N, D315N, W332F, and R67K. Each 50 μ L PCR reaction contained 200 μ M dNTP PCR mix (Promega), 1 X *Pfu* buffer, 125 ng of each primer (31 to 49 nt), 50 ng of *AllBP-6* plasmid DNA, and 2.5 units of *Pfu* polymerase. The nucleotide changes for each mutation as well as the associated PCR primers used, are outlined in Table 3. The thermocycle used for PCR followed program #2 with the exception of R67K and W332F which followed program #3.

The PCR products obtained were digested with *DpnI* at 37 °C for 2 to 4 hours. Competent XL1 Blue *E. coli* cells were electrotransformed with 5 to 8 μ L of the *DpnI*-digested PCR product. Plasmid DNA was amplified and purified from kanamycin-resistant colonies. Using homology primers upstream (T7 promoter primer) and downstream (Term) of the multiple cloning site of pET30a+ and, if necessary, an internal *allB* gene primer, *allB*-f, single primer PCR reactions were used to amplify sections of the gene for nucleotide sequencing. Nucleotide sequences were determined by gel electrophoresis performed by the Gene Technologies Lab at Texas A & M University on purified PCR products.

CREATION OF *E. coli* Δ *allB* KNOCKOUT STRAIN

A protocol very similar to the Wanner method (33) was used to insert the chloramphenicol-resistance gene, *cat*, into the *E. coli* genome in place of the *allB* gene.

Table 3: Mutagenesis primers

Mutant	WT codon 5' → 3'	PCR primer	PCR primer nucleotide sequence 5 → 3'
R67K	CGT	1	CCCATATTTCTGAACCGGGT <u>AAG</u> AGCCACTGGGAAGGTTATGAAACCGG
		2	CCGGTTTCATAACCTTCCCAGTGGCT <u>CTT</u> ACCCGGTTCAGAAATATGGG
C152A	TGT	1	GCTTCGTTGCGACC <u>GCT</u> GGCGATCGCGGTATCG
		2	CGATACCGCGATCGCC <u>AGC</u> GGTCGCAACGAAGC
C152S	TGT	1	GCTTCGTTGCGACC <u>AGT</u> GGCGATCGCGGTATCG
		2	CGATACCGCGATCGCC <u>ACT</u> GGTCGCAACGAAGC
C287A	TGT	1	CGGTA CTCTGGCGAAG <u>GCT</u> TCACCGCCGATCCGCG
		2	CGCGGATCGGCGGTGA <u>AGC</u> CTTCGCCAGAGTACCG
C287S	TGT	1	CGGTA CTCTGGCGAAG <u>AGT</u> TCACCGCCGATCCGCG
		2	CGCGGATCGGCGGTGA <u>ACT</u> CTTCGCCAGAGTACCG
D315N	GAC	1	CGACTGCCTGGTTTCC <u>AAC</u> CACTCTCCATGCC
		2	GGGCATGGAGAGTGGT <u>TGG</u> GAAACCAGGCAGTCG
S317A	TCT	1	GCCTGGTTTCCGACCAC <u>GCT</u> CCATGCCCGCCGG
		2	CCGGCGGGCATGG <u>AGC</u> GTGGTCGGAACCAGGC
W332F	TGG	1	CGGTAACATCATGAAAGCA <u>TTC</u> GGCGGTATCGCCGGTCTGC
		2	GCAGACCGGCGATACCGCC <u>GAA</u> TGCTTTCATGATGTTACCG

The BW25113/pKD46 *E. coli* strain had previously been obtained from the *E. coli* Gene Stock Center. The BW25113 strain can be transformed with linear DNA because it will not degrade the DNA, and pKD46 is a helper plasmid which contains the ampicillin resistance gene and the gene which codes for the λ Red recombinase. In the event that there is a linear piece of DNA which contains recognition sequences (FTR sites) flanked by homology sequences of a gene in the in the host genome, the recombinase will switch the genomic DNA between these two sites in exchange for the linear DNA between the same recognition sequences.

The linear DNA to transform was synthesized by PCR using the pKD3 plasmid as template DNA and the *Pfx* platinum polymerase kit. A stock of pKD3 was prepared from overnight cultures of LB/ampicillin inoculated with BW25113/pKD3 colonies. The pKD3 plasmid contained the *cat* gene flanked by FRT sites at the beginning and end of the gene. Two PCR primers were designed, H1P1 and H2P2. H1 was the 5' \rightarrow 3' homology sequence to the *E. coli* BW25113 genome -54 to -7 nucleotides prior to the ATG start codon of *allB*. H2 was homologous to the 3' \rightarrow 5' region +53 to +6 nucleotides after the *allB* gene. Directly after each homology sequence was a priming sequence, homologous to the 5' \rightarrow 3' region before the FRT site, P1, and to the 3' \rightarrow 5' region after the FRT site, P2. The FRT recombinase recognition sites flank the *cat* gene in pKD3. Each 50 μ L PCR reaction contained 2X *Pfx* buffer, 200 μ M dNTP PCR mix, 240 ng pKD3 plasmid template DNA, 0.4 μ M of each primer H1P1 and H2P2, 3X enhancer solution, 1.0 mM MgSO₄, and 2.5 Units *Pfx*. The PCR reaction was run under the thermocycle conditions of program #4. The presence of the expected PCR product

of 1130 base pairs was determined by 1% agarose gel electrophoresis with TAE buffer. The PCR product of two 50 μ L combined equivalent reactions was gel purified using the QIAquick gel extraction kit from Qiagen.

Single colonies of ampicillin-resistant BW25113 cells were used to inoculate 6 ml of SOB/ampicillin/1.0 mM L-arabinose media. The cells were made electrocompetent from small cultures by growth at 30 °C in LB/ampicillin until $OD_{600} \sim 0.5$, washed and stored by standard protocol. Five μ L of the gel purified ~ 1130 base pair PCR product was used to electrotransform 40 μ L of the BW25113 cells. After the transformation, the cells were grown at 37 °C for 1 hour followed by room temperature for 24 hours prior to growth on LB/chloramphenicol/1.0 mM L-arabinose solid media at 30 °C for 30 hours. The single colony obtained was used to inoculate three 6 ml LB/chloramphenicol liquid cultures grown overnight at 37 °C. One ml of this culture was used to isolate BWcam9 genomic DNA via Wizard[®] genomic DNA purification kit (Promega). The remaining BWcam9 cells were concentrated 100-fold with 10% glycerol for storage and used to inoculate LB/chloramphenicol and LB/chloramphenicol/ampicillin liquid cultures grown at 37 °C 12 hours to assess for loss of ampicillin resistance and retention of chloramphenicol resistance.

The isolated genomic DNA was used as template DNA for PCR reactions with combinations of 4 test primers. Two primers were internal gene primers of the *cat* gene, *camA* and *camD*. The *-allBK12* and *+allBK12* primers were homology sequences of the *E. coli* genome just before the H1 homology sequence and just after the H2 homology sequence, respectively. The Platinum *Pfx* polymerase kit was used to amplify DNA by

PCR in 25 μ L reactions: 1.3 units Pfx platinum polymerase, 1.0 mM MgSO₄, 200 μ M dNTP PCR mix, 3X enhancer solution, 140 ng genomic DNA, 2X Pfx amplification buffer, and 0.4 μ M each of two primers (camA/D; -/+*allBK12*; camD/+*allBK12*; camA/-*allBK12*; camD/-*allBK12*; camA/+*allBK12*). The thermocycle used was PCR program # 5 (Table 1). The nucleotide sequences of all primers used are summarized in Table 4. The PCR products were analyzed by 1% agarose gel electrophoresis in TAE buffer. The expected lengths of major DNA bands were calculated and compared to the results seen on the agarose gel.

CONVERSION OF *E. coli* Δ *allB* TO λ DE3 CELLS

The λ DE3 lysogenation kit from Novagen was used to convert the BWcam9 Δ *allB* knockout *E. coli* cells to DE3 cells for overexpression with the pET30 vector. The BWcam9 cells were used to inoculate 5 ml of LB/chloramphenicol/10 mM MgSO₄/0.2% w/v maltose, and grown at 37 °C to an OD₆₀₀ ~ 0.5. Five μ L of the liquid culture was mixed with 10⁸ plaque forming units (pfu) each of the λ DE3 prophage, selection phage, and helper phage to make a 21 μ L mixture. The mixture was incubated at 37 °C for 20 min, and diluted so that 0.4 μ L was incubated on solid LB/chloramphenicol media overnight at 37 °C.

Single colonies were used to inoculate 5-6 ml LB/chloramphenicol/10 mM MgSO₄/0.2% w/v maltose and grown until the OD₆₀₀ reached ~ 0.5. Two samples were made of 100 μ L each of the cell culture and 2 x 10³ pfu/ml T7 tester phage. The mixture was incubated at room temperature for 30 minutes, mixed with 3 ml of cooled top agarose and plated onto previously solidified LB or LB/0.4 μ M IPTG for overnight

Table 4: Primers used in construction of the *E. coli* $\Delta allB$ strain

Primer Name	PCR primer nucleotide sequence 5' → 3'
H1/P1	CCCGATATTGAACATTGAGTTAAAAACCAATCTGTATTTACAAGGAGGTGTAGGCTGGAGCTGCTTC
H2/P2	CACACCTTAACCGGAGAATGCCCGCCGCAAGGACGGGCATTGCAGGGGATGGGAATTAGCCATGGTCC
-allBK12	CGTCGCCTTTGCGGCCTACG
+allBK12	GGCTTTCGCGGCTGACTGC
camA	GGATATACCACGTTGATATATCCCAATGGC
camD	GCATCTGCCGACATGGAAGCC

growth at room temperature. The rest of the LB/chloramphenicol/10 mM MgSO₄/0.2% w/v maltose cultures at OD₆₀₀ ~ 0.5 were used to make frozen cell stocks (600 μL cell culture combined with 400 μL sterile 75% glycerol). Electrocompetent stocks of the frozen permanents were made by standard procedure and used to overexpress *allB* mutants in pET30a+.

METAL REMOVAL FROM ZnALN AND CoALN AND RECONSTITUTION

ZnALN was treated with 7.0 mM dipicolinate in a solution of 50 mM MES, 500 mM Na₂SO₄, 0.5 mg/ml ZnALN, pH 6.0. The 150 mM dipicolinate stock was in ethanol, the control solution contained 4.6% v/v EtOH but without dipicolinate. Each sample was stored on ice and its activity assessed 0.1, 2, 8.25, 22, 29.5, 40, and 53.5 hours after the addition of dipicolinate. After approximately 55 hours of treatment with dipicolinate, the solution was brought to pH 8.1 with 500 mM HEPES, pH 8.1. The dipicolinate was removed by a series of concentration and dilution steps, using the YM30,000 Milipore filter and the Amicon filtration apparatus, until the concentration of dipicolinate was calculated to be 0.14 nM. The concentration of dipicolinate after each concentration and dilution step was determined by the multiplying the previous dipicolinate concentration by the quantity of (concentrated volume/diluted volume). Atomic absorbance analysis was performed on the chelated ZnALN after the removal of dipicolinate and PD-10 elution.

CoALN was treated with 25 mM dipicolinate, 50 mM PIPES, pH 6.5, for 30.5 hours on ice. The dipicolinate was then removed in the same fashion as for ZnALN as was the AA analysis sample preparation. Apo enzyme from CoALN was also prepared

in the presence of the reducing agent sodium dithionite. In this case, all buffers were degassed with argon. The 13 ml chelation solution consisted of 1.0 mg/ml CoALN (650 μ L), 2.0 mM $\text{Na}_2\text{S}_2\text{O}_4$, 50 mM PIPES buffer, and 25 mM dipicolinate (no EtOH), pH 6.5. The enzyme and $\text{Na}_2\text{S}_2\text{O}_4$ were added after the other contents had been degassed with argon for \sim 2 hours. After 40 hours on ice, the solution was dialyzed in 500 ml of degassed exchange buffer (50 mM HEPES, pH 8.1) twelve hours. The chelation solution was dialyzed an additional 4 times for 12 hours each at \sim 8°C. The $\text{Na}_2\text{S}_2\text{O}_4$ was added freshly to the buffer for each exchange to a final concentration of 2.0 mM.

An attempt was made to reconstitute the Apo ALN (from CoALN) enzyme with Zn at pH 6.5, 7, 7.5, and 8. The reconstitution solution consisted of 1 mg/ml enzyme, 100 μ M ZnCl_2 , 50 mM buffer (pH 6.5, 7: PIPES; pH 7.5, 8: HEPES), and 50 mM KHCO_3 . The control was the same mixture without the KHCO_3 . The activity of the samples was checked after 18 hours incubation on ice. The Apo enzyme obtained from CoALN was also treated with 100 μ M ZnCl_2 or MnCl_2 with or without 50 mM KHCO_3 at pH 8.0 on ice. The activity was checked after 24 hours.

RESULTS

CLONING AND OVEREXPRESSION OF *allB*

The *allB* gene was cloned into the pET30a+ vector in order to obtain more efficient overexpression over that of pMU-6. The agarose gel in Figure 4 shows that the unpurified, purified, and *EcoRI/NdeI*-digested PCR product obtained from the AllBpET30a and PBSA₂ primers and pMU-6 template DNA was between 1,000 and 1,500 base pairs in length. The *allB* gene is 1362 nucleotides. Electrotransformation of XL1 Blue *E. coli* cells with the ligation product resulted in kanamycin-resistant colonies. The plasmid DNA amplified and isolated from selected colonies contained the sequence of *allB* in the appropriate region of the plasmid. The *allB* gene was overexpressed very well in *E. coli*. The SDS PAGE of *E. coli* whole cell contents, in the presence of β -mercaptoethanol, after overexpression of *allB*, presented in Figure 5, shows that allantoinase was the predominant protein.

ENZYME PURIFICATION

Allantoinase was successfully purified by ammonium sulfate precipitation from the soluble cell lysate material and size exclusion chromatography. Figure 6 shows the purity of ALN over the progression of the purification protocol used to purify the wild type allantoinase and associated mutants. The allantoinase activity and protein yield progressions for S317A ZnALN are presented in Table 5. The specific activities of all purified allantoinase enzyme samples are summarized in Table 6 along with the metal content as determined by atomic absorbance. The H316A and H316N mutants were not obtained because allantoinase could not be found in any of the gel filtration fractions and

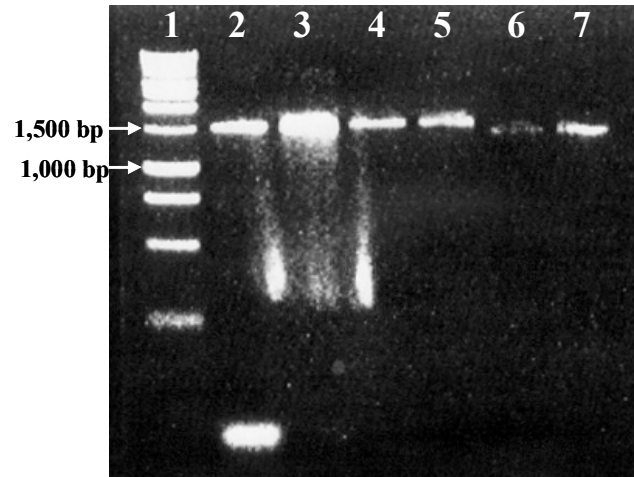


Figure 4: Agarose analytical gel for cloning of *allB*. Lane 1: 1 kilobase ladder, Lane 2: unpurified PCR product, Lane 4: purified PCR product, lane 6: *EcoRI/NdeI* double digested PCR product.



Figure 5: SDS PAGE of *allB* overexpressed in *E. coli*. Lane 1: ALN reference, Lane 2: crude cells of *allB*/pET30 overexpression BWcam9/ λ DE3.

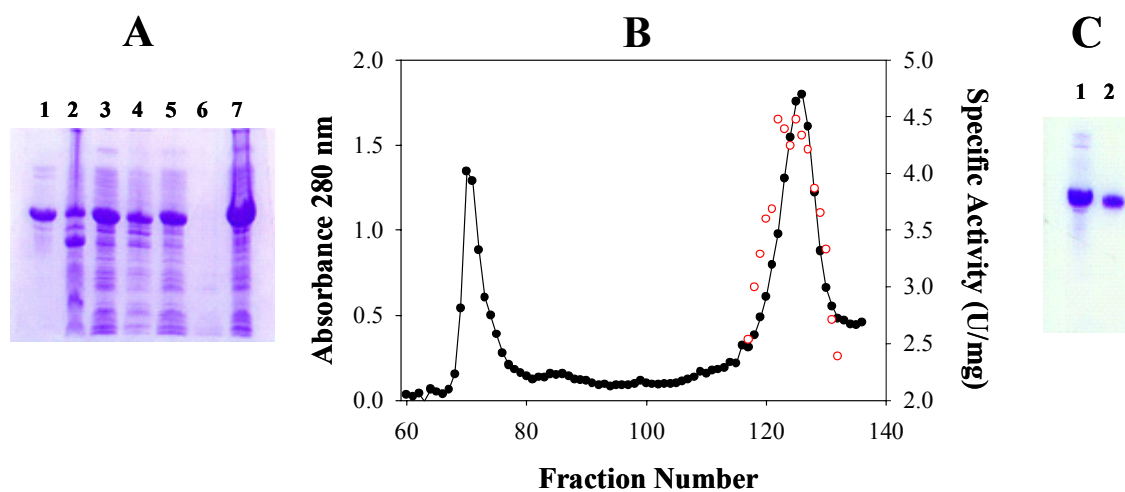


Figure 6: Sample purification of allantoinase represented by the S317A mutant. **A)** Lane 1: sample A ALN reference, Lanes 2-7: sonication pellet, sonication supernatant (S/N), 0-20% ammonium sulfate (A.S.) pellet, 0-20% A.S. S/N, 20-50% A.S. S/N, and 20-50% A.S. pellet, respectively. **B)** A34 Column chromatography separation profile of 20-50% A.S. pellet where black circles indicate the absorbance at 280 nm of each fraction and open red circles are the specific activities of select fractions. **C)** Lane 1: sample A ALN reference, Lane 2: purified S317A ZnALN mutant.

Table 5: Purification summary of S317A allantoinase activity

Purification Step	Volume (mL)	mg Protein	Total Units	Specific Activity (U/mg)
<i>Sonication Supernatant</i>	62	1220	1360	1.1
<i>20-50% Ammonium Sulfate Pellet</i>	17	740	1290	1.7
<i>Pooled A34 gel filtration fractions</i>	74	160	703	4.5

Table 6: Activity, metal content and protein yield of purified allantoinase samples

Purified Enzyme Sample	Equivalents of Divalent Cation per subunit			Specific Activity U/mg	Protein Yield (mg)	mass cells (g)	g cells per L
	Zn	Co	Mn				
A*	0.06	—	—	0.09	1000	40	10
B*	0.5	—	—	2	34	10	5
D ZnALN*	0.1	—	—	0.38	296	17.3	8.7
E*	0.08	—	0.2	0.9	378	17.5	8.8
F ZnALN*	1.1	—	—	3.9	40	61.2	20
G Zn ALN*	1.4	—	—	6	217	37.7	7.5
H ZnALN*	1.8	—	—	10	23	7	7
CoALN*	0.08	1.6	—	66	116	9	9
MnALNa*	0.7	—	0.8	20	290	26.6	13.3
MnALNb*	0.3	—	1	27	302	33.3	16.5
R67A	2.1	—	—	0.18	36	16.4	5.5
C152A	1.7	—	—	6.2	97	12.6	6.3
C152S	1.8	—	—	4.4	80	10	5
C287A	1.5	—	—	0.5	91	13.4	4.5
C287S	2.2	—	—	3.3	81	12	4
D315N	1.4	—	—	0	244	12.7	12.7
S317A	1.4	—	—	4	157	11.3	11.3
W332F	1.4	—	—	1	160	15.4	5.1

* Wild type allantoinase

the sonication supernatant and 50% ammonium sulfate pellet did not have activity.

These two mutants did not overexpress as well as the other mutants.

CONSTRUCTION OF *E. coli* $\Delta allB$ λ DE3 KNOCKOUT STRAIN

Before *allB* mutants could be overexpressed in *E. coli*, an *E. coli* $\Delta allB$ knockout strain had to be constructed to prevent the synthesis of background WT allantoinase.

The protocol of Wanner was used to replace the *allB* gene in the *E. coli* genome with the chloramphenicol resistance gene. The PCR product, *cam9*, obtained from the pKD3 template and the primers H1/P1 and H2/P2 was the expected size of 1130 base pairs—slightly greater than 1,000 base pairs and less than 1,500 base pairs as shown in Figure 7A. Electrotransformation of the gel purified PCR product with BW25113/pKD46 competent cells resulted in one chloramphenicol-resistant colony, BW*cam9*. The isolated cells lost ampicillin resistance by growing cell stocks of this colony at 37 °C in LB/chloramphenicol. The PCR reactions performed with the BW*cam9* genomic DNA template and the combinations of test primers, Table 4, resulted in several PCR products. However, for each sample, one PCR product was of significantly higher concentration. The major PCR product for each set of test primers, presented in Figure 7B were considered to be the expected size based on their electrophoretic migration. The expected DNA band lengths for each PCR reaction using combinations of test primers with BW*cam9* DNA template are summarized in Table 7.

Overexpression with pET30a+ is accomplished using T7 RNA polymerase for more highly efficient transcription over the *E. coli* RNA polymerase. The T7 promoter

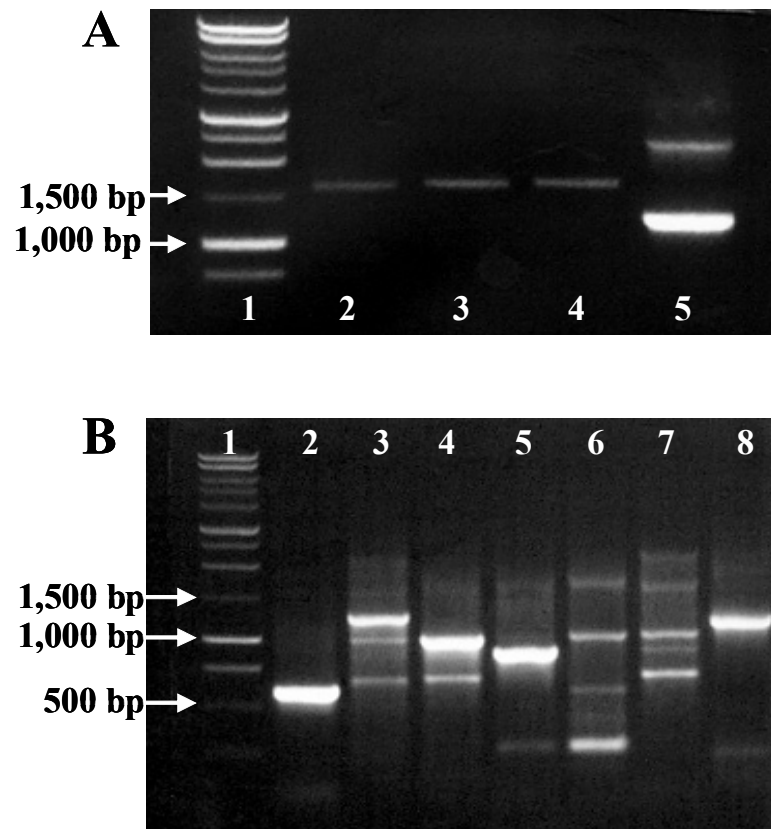


Figure 7: Agarose analytical gels for construction of *E. coli* $\Delta allB$. **A)** & **B)** Lane 1: 1 kilobase ladder. **A)** Lanes 2-5: pKD3 mini-prepped plasmid, Lane 5: cam9 gel purified PCR product. **B)** Lanes 2-5: BWcam9 genomic DNA template PCR products #1-4, Lane 8: PCR product #5.

Table 7: Expected PCR products for test PCR reactions from *E. coli* $\Delta allB$ DNA

BWcam9 Test PCR product #	Primer 1	Primer 2	Anticipated PCR product length (bp)
1	camA	camD	649
2	- <i>allB</i> K12	+ <i>allB</i> K12	1248
3	camD	+ <i>allB</i> K12	985
4	camA	- <i>allB</i> K12	848
5 (<i>pKD3</i> DNA template)	H1P1	H2P2	1130

is not present in the *E. coli* genome. The protocol for the λ DE3 lysogenation kit is based on a published procedure (34) where *E. coli* are infected with a λ phage that has been genetically engineered. The altered λ phage has the T7 RNA polymerase gene inserted into the *int* gene. The *int* gene is required for the integration of the phage into the host genome, and therefore, the phage cannot kill the cells. Chloramphenicol-resistant colonies were obtained from LB/chloramphenicol solid media plated with the BWcam9 cells/ λ DE3/selection phage/helper phage lysates incubation mixture. The growth of the selected colony in LB containing chloramphenicol/maltose/10 mM MgSO₄, and subsequent mixture with the T7 tester phage, resulted in plaque formations when plated on LB and LB/IPTG. More plaques were obtained on the LB/IPTG media. The SDS/PAGE gel shown in Figure 5 also demonstrates that the BWcam9/ λ DE3 cells were able to overexpress *AllBP-6*.

EFFECTS OF DIVALENT CATIONS

Allantoinase sample A, purified from pBS+, was assayed in the presence of different divalent cations because the enzyme is thought to be metal-dependent. As summarized in Table 8, activity enhancement was achieved with MnCl₂, CoCl₂ and NiCl₂ compared to the specific activity of 0.09 units/mg obtained in the absence of divalent cation. Cadmium chloride and ZnCl₂ did not enhance the activity. Since Mn resulted in the greatest improvement, purified enzyme samples B, D, and E were assayed in 25 μ M MnCl₂. The Zn content of these samples varied. Samples D and E were purified from overexpression in *E. coli* cultured in TB media containing 250 μ M ZnCl₂ and MnCl₂, respectively. Sample B contained 0.5 equivalents of Zn. Table 9 shows the

Table 8: Specific activity (U/mg) of sample A ALN assayed with Co, Mn and Ni

Divalent Cation	Concentration of Divalent Cation in Assay			
	25 μM	50 μM	100 μM	500 μM
Co	0.46	0.46	0.5	1.8
Mn	3.5	3.7	4	ND
Ni	0.11	0.11	0.1	0.13

ND value not determined

Table 9: Varying enhancement of different purified samples of ALN by Mn

Enzyme Sample	Enzyme Equivalents		Specific Activity (U/mg)	
	Zn	Mn	no Mn	25 μ M MnCl ₂
A	0.03	0.01	0.09	3.1
B	0.5	ND	2	1.6
D	0.1	ND	0.38	2.44
E	0.08	0.2	0.91	1.1

ND value not determined

specific activity of these purified enzyme samples with and without Mn in the assay as well as the Zn and Mn content of the purified enzyme.

DETERMINATION OF THE AMOUNT OF ALLANTOIN CONSUMED

It has been stated in the literature that allantoinases can vary in their stereoselectivity for S or R-allantoin (2, 3). Manganese-supplemented assays with sample A were allowed to progress until the absorbance at 340 nm no longer increased. The addition of more enzyme did not cause the A_{340} to increase again; the enzyme was not losing activity with time. Figure 8 shows the A_{340} , calculated from a 1:10 dilution of each time point, versus time after the addition of allantoinase to 6, 8, 10 and 18 mM allantoin. The maximum A_{340} reached at each allantoin concentration was estimated. Approximately 46-50% of the allantoin was consumed as determined by dividing the observed A_{340} value by the expected A_{340} for 100 % conversion of allantoin to allantoic acid at each allantoin concentration.

Mn-CULTURED OVEREXPRESSION OF *allB*

Growth experiments for *E. coli/allBpET30a+* in the presence of Mn were performed to determine if there were better conditions, combination of temperature and IPTG concentration, for the production MnALN with little Zn contamination. The Mn enzyme was more active, and therefore, it was predicted that the higher the enzyme activity, the higher the content of Mn vs. Zn. The progression of enzymatic activity of crude cell extracts of the first Mn-culture growth experiment is shown in Figure 9A-C for the determination of which temperature and approximate concentration of IPTG to use. Figure 9D is a summary of the second growth experiment where the concentration

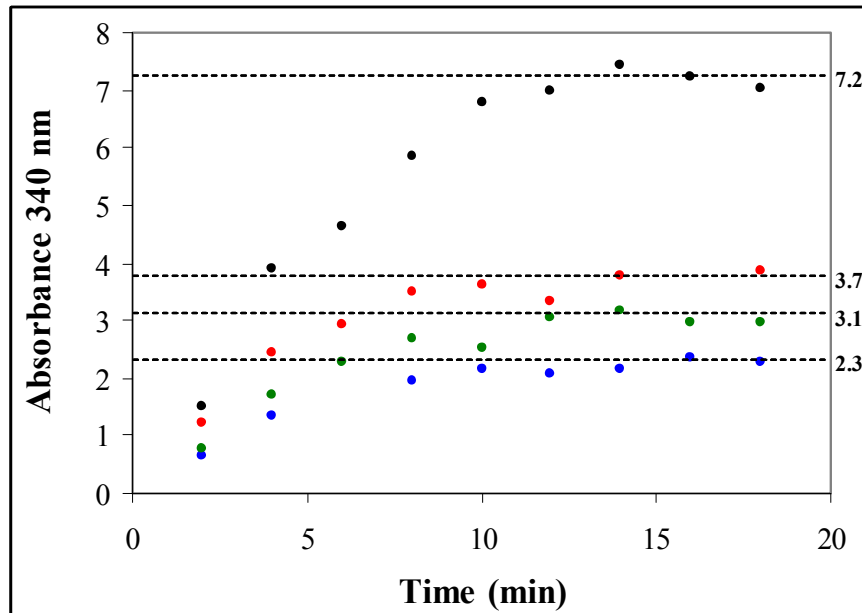


Figure 8: Allantoinase assayed in presence of Mn until the A_{340} no longer increased. Blue, green, red, and black circles represent 6, 8, 10, and 18 mM allantoin, respectively. Horizontal dashed lines represent the approximate maximum absorbance values.

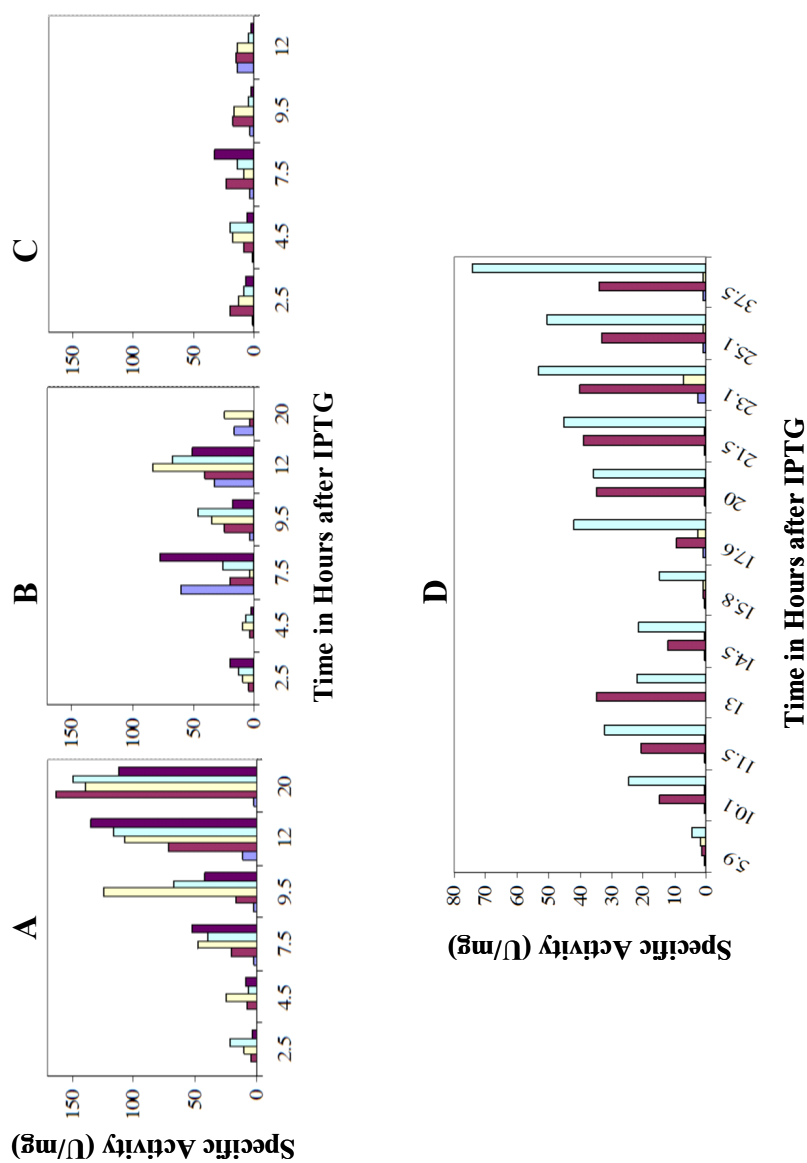


Figure 9: Activity progression of Mn-cultured overexpression of *allB*. (Top) Progression of activity over time after the addition of varying amounts of IPTG (no IPTG: blue, 50 μM: maroon, 100 μM: yellow, 250 μM: turquoise, 500 μM: purple) at **A**) room temperature (20°C), **B**) 30°C, and **C**) 37°C. Bottom: second Experiment **D**) of activity over time after addition of varying amounts of IPTG with or without the presence of 3 mM MnSO₄ in the culture 25 μM IPTG/no Mn: blue, 25 μM IPTG/Mn: maroon, 50 μM IPTG/noMn: yellow, 50 μM IPTG/Mn: turquoise.

of IPTG to use and length of time to grow the cells was determined. These two experiments were the basis for the production of a second MnALN sample, MnALNb, where crude cell extract activities from a 1 L culture were monitored over time. The MnALNb sample had a specific activity of 27 U/mg and 1.0 equivalent of Mn per subunit. The activity and AA analysis results for MnALN are summarized in Table 6 of all proteins purified.

pH RATE PROFILES

The pH dependence of catalytic activity was used to identify potentially interesting amino acids for further investigation, based on the pH values at which activity decreases from the maximal value. The pH rate profiles for ZnALN, CoALN and ALN in presence of MnCl₂ showed that activity was pH-dependent. The data followed a bell-shaped pattern with pK₁ and pK₂. The bell-shaped curves are shown in Figure 10 for log (k_{cat}/K_M) vs. pH from fits of the data to equation 3. The pK₁ for ALN in the presence of MnCl₂, ZnALN, CoALN and were 7.8, 5.3 ± 0.09 and 5.7 ± 0.07, respectively. The pK₂ values for ALN assayed with MnCl₂ and CoALN were both 8.9 (8.9 ± 0.06 for CoALN), and the pK₂ for ZnALN was 8.7 ± 0.05. The standard deviations were not determined for Mn profile because the pK₁ and pK₂ values were too close—the data did not converge to give K₁ and K₂ in the program used. Sigma plot was then used to try and fit the data to equation 3 and the values for K₁ and K₂ used in the last iteration were used as the value for K₁ and K₂ without a value for standard deviation. As seen in Figure 11, the parameters obtained fit the data nicely; however, in the final output, Sigma plot does not give values which would correspond to a pK_a.

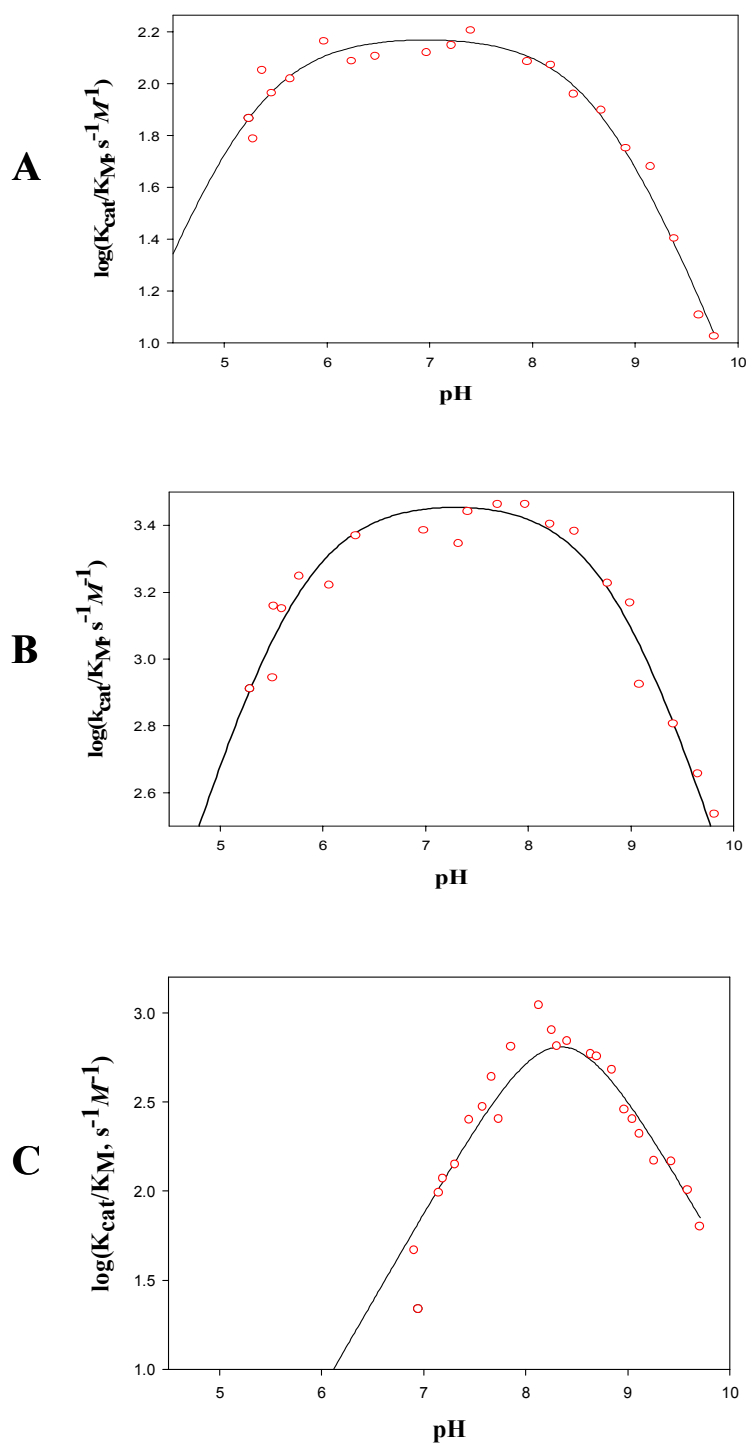


Figure 10: pH rate profiles of Zn, Co and Mn allantoinase. The $\log(k_{cat}/K_M)$ data for **A)** ZnALN **B)** CoALN **C)** ALN in presence of $25 \mu\text{M}$ MnCl_2 fit to equation 3 as a function of pH.

DIPICOLINATE TREATMENT OF Zn AND Co ALLANTOINASE

The activity of ALN was dependent on the presence of divalent cations. Moreover, the pK_1 values appeared to be dependent on the specific metal ion present. There was an interest in being able to obtain allantoinase with bound Zn, Co, Ni, or Mn in order to determine pK_1 and pK_2 , the number of equivalents of metal at maximum activity, and to obtain electron paramagnetic resonance spectra in the case of MnALN. Dipicolinate was used to make apoALN from ZnALN and CoALN, with and without a reducing agent, under conditions of reduced pH. A visible amount of white precipitate was seen during the metal removal for ZnALN, but was not visible by the completion of the dipicolinate removal. The activity of ZnALN continued to decrease up to 40 hours while being treated with 7 mM dipicolinate at pH 6.0 as shown by the activity progression in Figure 11. However, AA analyses showed that there was a significant amount of Zn present in the sample compared to the metal-free buffer. Cobalt ALN could be treated at a higher pH, and the activity diminished more quickly. Precipitate was not seen for either of the two treatments of CoALN with dipicolinate. AA analyses (Table 10) showed that in the absence of $Na_2S_2O_4$, the Co was efficiently removed as well as some of the Zn contamination. AA analyses for CoALN treated with dipicolinate in the presence of $Na_2S_2O_4$ was considered to be unreliable because the linear regression parameters for the Zn and Co standards were considerable different from the values normally obtained. The metal removal from CoALN was repeated in sodium dithionite in case the oxidation of cysteine residues was preventing reconstitution of apoALN.

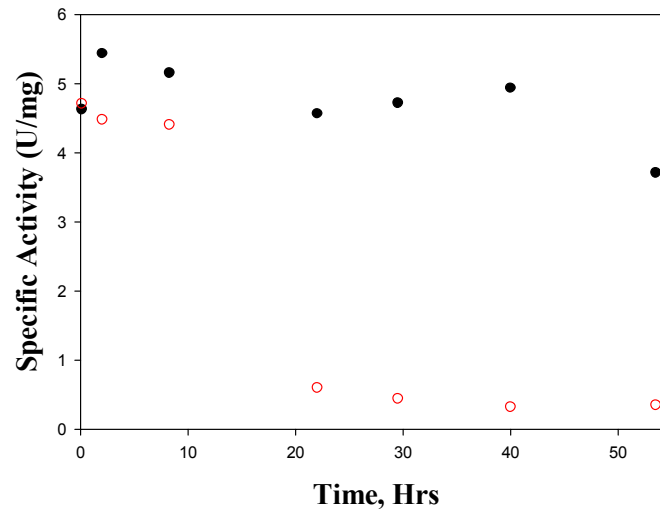


Figure 11: Activity progression of ZnALN specific activity during metal removal. Specific activity of allantoinase without dipicolinate is represented by black circles and by open red circles while treated with 7 mM Dipicolinate.

Table 10: Metal content of dipicolinate-treated ZnALN and CoALN

Dipicolinate-Treated Enzyme	Concentration μ M			Equivalents		Dilution Buffer	
	Enzyme	Zn	Co	Zn	Co	μ M Zn	μ M Co
ZnALN	2	6.71	NM	3.4	NM	0.11	NM
CoALN	15.9	0.5	ND	0.03	0	ND	ND
CoALN ^a	8.7	NM	ND	NM	0	2.7	ND
CoALN ^a	4	26	NM	6.4	NM	2.7	ND

^a Dipicolinate treatment in the presence of 2 mM Na₂S₂O₄

ND no metal (Zn or Co) detected

NM not measured

RECONSTITUTION OF apoALN

Attempts to reconstitute samples of apoALN obtained from CoALN with and without $\text{Na}_2\text{S}_2\text{O}_4$ were not successful. The activity of both enzyme samples did not increase beyond their initial value at any of the pH conditions or in the presence of bicarbonate. The activity actually decreased at pH 6.5 and 7.0. For apoALN obtained in the presence of $\text{Na}_2\text{S}_2\text{O}_4$, enzyme activity was barely detectable after 24 hour incubation with Mn or Zn (Table 11).

STRUCTURAL MODEL OF ALLANTOINASE

Of all amidohydrolase enzymes, L-hydantoinase has the highest amino acid sequence identity to allantoinase (37 %), and both enzymes cleave the same type of bond. Dihydroorotase has low sequence homology to ALN (8 %), but the DHO crystal structure of the enzyme has the dihydroorotate molecule present (12). Figures 12 and 13 show the amino acid sequence alignments of allantoinase with LHYD and DHO, respectively. As depicted in Figure 14, allantoin, hydantoin and dihydroorotate have a common $(\text{—NH[CO]—})_2$ motif. The 3D structural model shown in Figure 15 was constructed with allantoin present via sequence alignments and structural overlays with dihydroorotase (12) and L-hydantoinase crystal structures (26). From the hypothetical ALN structure tethered to the DHO structure by conserved histidine residues, it was determined that the following residues, depicted in Figure 15C, could be in the vicinity of the substrate: R67, C152, C287, S317, S288, D315, W332, G333, G334. Arginine 67 is a conserved cationic amino acid and the only arginine in the vicinity of the active site according to the model. Histidine 316 is another completely conserved amino acid. All

Table 11: Specific activity for reconstitution of apoALN in the presence and absence of $\text{Na}_2\text{S}_2\text{O}_4$

Sample	100 μM Metal	Time Hours	pH 6.5		pH 7.0		pH 7.5		pH 8.0	
			no KHCO_3	50 mM KHCO_3	no KHCO_3	50 mM KHCO_3	no KHCO_3	50 mM KHCO_3	no KHCO_3	50 mM KHCO_3
apoALN no $\text{Na}_2\text{S}_2\text{O}_4$	Zn	0	0.26	0.26	0.34	0.27	0.31	0.2	0.3	0.3
apoALN no $\text{Na}_2\text{S}_2\text{O}_4$	Zn	18	0.09	0.17	0.1	0.24	0.17	0.29	0.44	0.34
apoALN $\text{Na}_2\text{S}_2\text{O}_4$	Mn	24							0.04	0.03
apoALN $\text{Na}_2\text{S}_2\text{O}_4$	Zn	24							0.02	0.01


```

LHYD 1  -MFDVIVKNCRLVSSDGITEADILVKDGKVA AISADTS DVEASRTI DAGG
ALN 2   MSFDLI IKNGTVILENEARVV DIAVKG GKI AAI GQDLG--DAKEVMDASG
          ** * **          ** ** ** ** *      *      ** *

LHYD 50  KFVMPGVVDEH VHI IDMDLKNRYGRFELDSESAAVGGITTI IEMPITFPP
ALN 49  LVVSPGMVDAHTHI SEPGRSHWEG- YETGTRAAAKGGITTTMIEMPLNQLP
          * ** ** * **          * *      ** **** ** ** *

LHYD 100 TTTLD AFLEKKKQAGQ-RLKVDFALYGGVPGNLP EIRKMHDAGAVGFXS
ALN 98  ATVDR ASI ELKFDA AKGLTIDAAQLGGLVSYNIDRLHELDEVG VVGFKC
          * * * * *      * * * ** * *      *      * ****

LHYD 149 MMAAS----VPGMFDAVSDGELFEIFQEIAACGSVIVVH AENETI IQALQ
ALN 148 FVATCGDRGIDNDFRDVNDWQF FKG AQKLGELGQPVLVH CENALICDELG
          *          * * * * *      *      * ** ** * *

LHYD 195 KQIKAAAGKDMAAYEASQPVFQENEAIQRALLLQKEAGCRLIVLH VSNPD
ALN 198 EEAKREG RVT AHDYV ASRPVFTVEAIRRVLYLAKVAGCRLHVCHVSSPE
          * *          * ** ** * ** * ** * * * ** ** * ** *

LHYD 245 GVELIHQAQS EGQDVHCESGPQYLNITTD DAERIGPYMKVAP PVRSAEMN
ALN 248 GVEEVTRARQ EGQDVT CESCPHYFVLDTDQFEEIGTLAKCS PPIRDL ENQ
          ***      * ** ** ** ** * *      ** * ** * ** * *

LHYD 295 IRLWEQLENGLIDTLGSDHGGHPVEDKEPGWKDWWKAGNGALGLETS LPM
ALN 298 KGMWEKLFNGEIDCLVSDHSPCPPEMKAG---NIMKAWGGIAGLQSCMDV
          ** * ** ** * ** ** * ** *      * ** *      ** * **

LHYD 345 MLTNGV NKGRLSLERLVEVMCEKPAKLFGIYPQKGT LQVGS DADLLILD L
ALN 345 MFDEAVQKRGMSLPMFGKLMATNAADIFGLQ-QKGR IAPGKDADFVFIQP
          *      * * ** *      *      * ** ** ** * ** **

LHYD 395 DIDTKVDASQFRSLHKYSPFDGMPVTGAPVLT MV RGT VVAEKGEVLVEQG
ALN 394 NSSYVLTND DLEYRHKVSPYV GRTIGARITK TILRGDVIYDIEQGFVPAP
          ** ** *          *      ** *

LHYD 445 FQGFVTRRN YEASK
ALN 444 KGQFILKHQQ----
          ***

```

Figure 12: CLUSTALW amino acid sequence alignment of *E. coli* ALN and LHYD from *Arthobacter aurescens*. Identical residues are neon blue with asterisks, Zn ligands are highlighted in magenta, and X represents a carboxylated lysine residue.

```

DHO   4          SQVLKIRRPDDWHLHLLRDG---DMLKTVVP-YTS
ALN  36  DLGD--AKEVMDASG---LVVSPGMVDAHTHISEPGRSHWE-G-YETG-T
                                     * * *

DHO   34  E----I-YGRAIVMPNLAPPVTTVEAAVAYRQRILDAVPAPHDFTPLMTC
ALN   78  RAAAKGGITTMIEMPLNQLPATVDRASIELKFDAAKGKL-T--IDAAQLG
                                     * ** * * *

DHO   79  YLTDSLD-PNELERGFNEGVFTAAXLYPANATT----NSSHGVTSVDAIM
ALN  125  GLVS--YNIDRLHELDEV-GVVGFKCFVATCGDRGID-NDFRDVNDWQFF
      *          *          *          *

DHO  124  PVLERMEKIGMPLLVHGEVTHADI-----DIF-
ALN  171  KGAQKLGELGQPVLVHCENAL---ICDELGEEAKREGRVTAHDVASRPV
      * * * * *

DHO  151  DREARFIESVMEPLRQRLTALKVVFEHITTK-DAADYVRDGN---ERLAA
ALN  218  FTEVEAIRRV-LYLAKVAGC-RLHVCHVSS-PEGVEEVTRARQEGQDVTC
      * * * *          *          *

DHO  197  TITPQHLMFNRNHMLVGGVRPHLYCLPILKRNIHQQALRELVASG-FQRV
ALN  265  ESCPHFVLDTDQF-EEI-GTLAKCSPIRDLENQKMWEKLFNGEI-D-
      *          * *          *          *

DHO  246  FLGTDSAPHARHRKE--SSCG---CAGCFNAPTALGSYATVFEE-MNALQ
ALN  311  CLVSDHSPCPPEMKAG---NIMKAWGIAGLQSCMDVMFDEAVQK-RGMS
      * * *          *

DHO  289  --HFEAFCSVNGPQFYGL--P-VND-----TFIELVREEQQVAESIALT
ALN  357  LPMFGKLMATNAADIFGLQ-QKGRIAPGKDA-----
      *          *          **

DHO  328  DDTLV-----PFLAGETVRW-SVK
ALN  386  -----DFVFIQPNSSYVLTNDDLEYRHKVSPYV--GRTIG-ARITKTILR

ALN  429  GDVIYDIEQGFPVAPKGQFILKRNYEASK

```

Figure 13: Amino acid sequence alignment of ALN and DHO from *E. coli*. Identical residues are neon blue with asterisks, Zn ligands are highlighted in magenta, and X represents a carboxylated lysine residue.

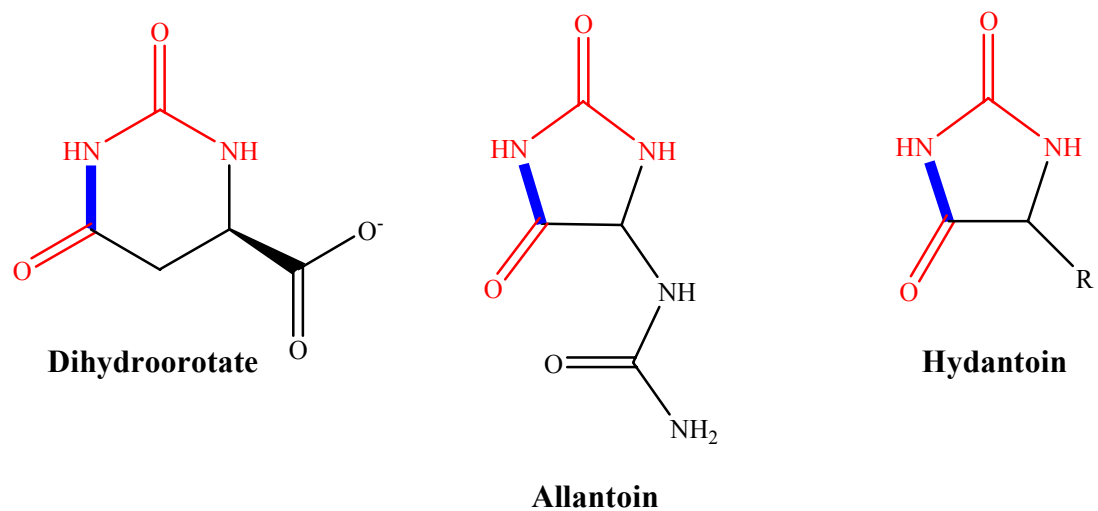


Figure 14: The substrates for dihydroorotase, allantoinase and hydantoinase. The substrates for dihydroorotase, allantoinase and hydantoinase are pictured from left to right, respectively. The bond cleaved by each enzyme is highlighted in blue, and the similar structural motif is highlighted in red.

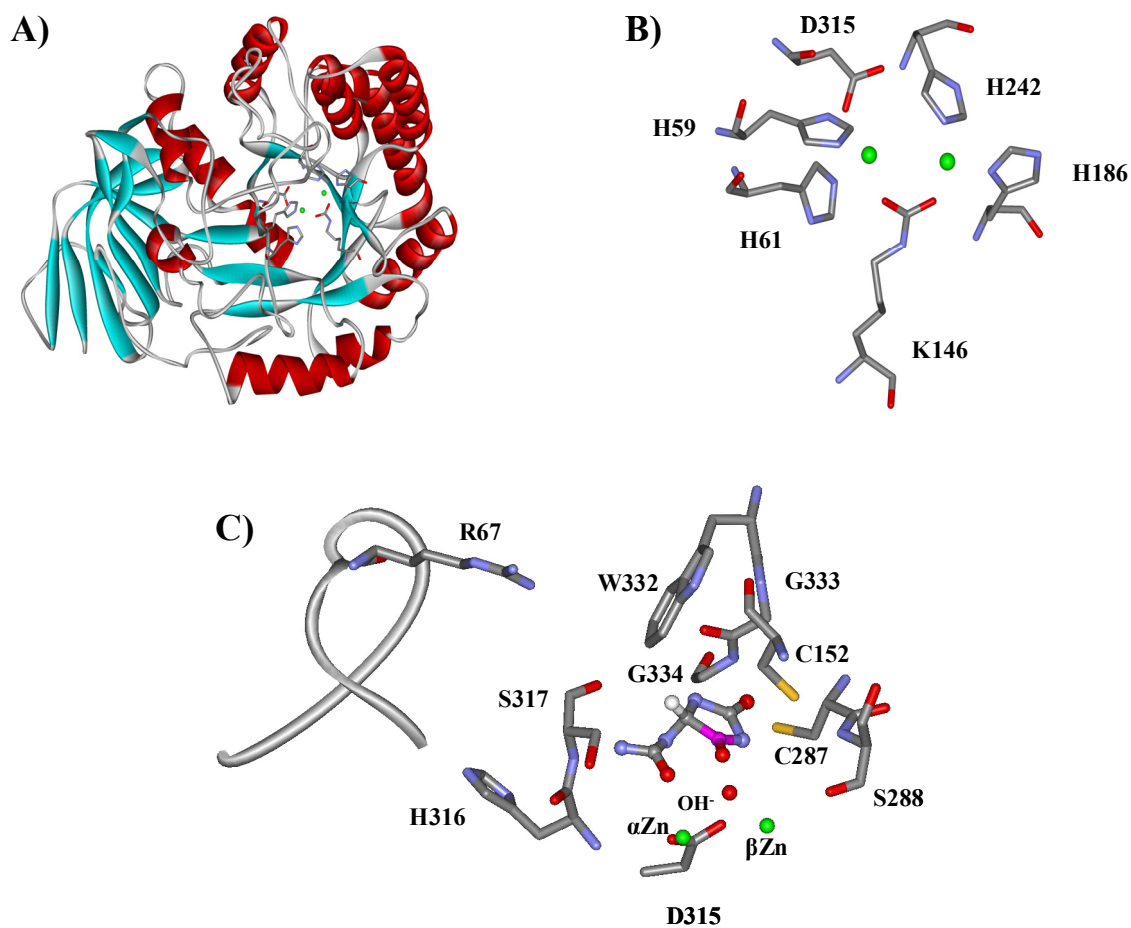


Figure 15: Representations of the structural model of ALN. **A)** Hypothetical 3D structural model of allantoinase and **B)** Predicted Zn ligands of allantoinase and **C)** Residues of allantoinase which might contact allantoin (ball and stick) where nitrogen, carbon, oxygen and Zn are represented in blue, grey, red and green, respectively.

of these residues are completely conserved in ALNs with the exception of C152 and S288. However, in the allantoinase alignment, and in other BLAST search alignments, the *E. coli* C152 position appears to be a serine otherwise. The C287 residue is not only conserved in the allantoinase alignment, but also in all putative allantoinases found from a BLAST search using the *E. coli* ALN sequence. Aspartic acid 315 was the closest residue in proximity of the bond which is cleaved by ALN, and accordingly was proposed to be the residue involved in an acid/base catalysis mechanism based on previous work for dihydroorotase (12).

SITE-DIRECTED MUTAGENESIS

The structural model and allantoinase amino acid sequence alignments were used as the basis for the amino acids selected for site-directed mutagenesis. The mutations chosen for mutagenesis were R67K, C152S, C152A, C287S, C287A, D315N, H316N, H316A, and W332F. The H316N mutation was as a more conservative mutation over H316A due to the problems obtaining the H316A mutation during purification and the poor overexpression of H316A. The method of QuickChange[®] mutagenesis was successfully used to synthesize the complete *allB*/pET30a vector. The PCR products, obtained from WT *allB*/pET30 template DNA and the primers outlined in Table 3, were between 6,000 and 8,000 base pairs according to agarose gel electrophoresis. Competent XL1 Blue *E. coli* cells electrotransformed with the *DpnI*-digested PCR products were able to ligate the linear PCR products and kanamycin-resistant colonies were obtained. Multiple copies of plasmid DNA were isolated and their nucleotide sequences confirmed to match the expected sequence for each desired mutant.

KINETIC PARAMETERS FOR WT AND MUTANT ALLANTOINASES

In order to determine the affects of each mutation on substrate binding and catalysis, the catalytic efficiency, k_{cat}/K_M , or additionally, K_M and k_{cat} for WT allantoinase and associated mutants were calculated from plots of velocity vs. allantoin concentration data at pH 8.0. When the relationship between velocity and allantoin concentration could be fit to equation 1 with low error, all three kinetic parameters were determined. When the relationship was linear, equation 1 was inappropriate and equation 2 was used to determine k_{cat}/K_M . The velocity versus allantoin concentration plots are shown in Figure 16 for wild type ZnALN, sample A ALN in the presence of MnCl_2 and allantoinase mutants R67K, C152A, C152S, C287A, C287S, S317A, and W332F. The kinetic parameters obtained from the plots in Figure 16 are summarized in Table 12. At room temperature, allantoin does not stay in solution for extended periods of time at concentrations of ~ 40 mM and above. Therefore, data sets were obtained in the concentration range of 5-45 mM and 5-70 mM allantoin so that the set at lower concentrations of allantoin could be used in the event that the substrate precipitated at the higher concentrations. Activity for the D315N mutant was not detectable using up to 0.95 mg/mL of ALN in the assay.

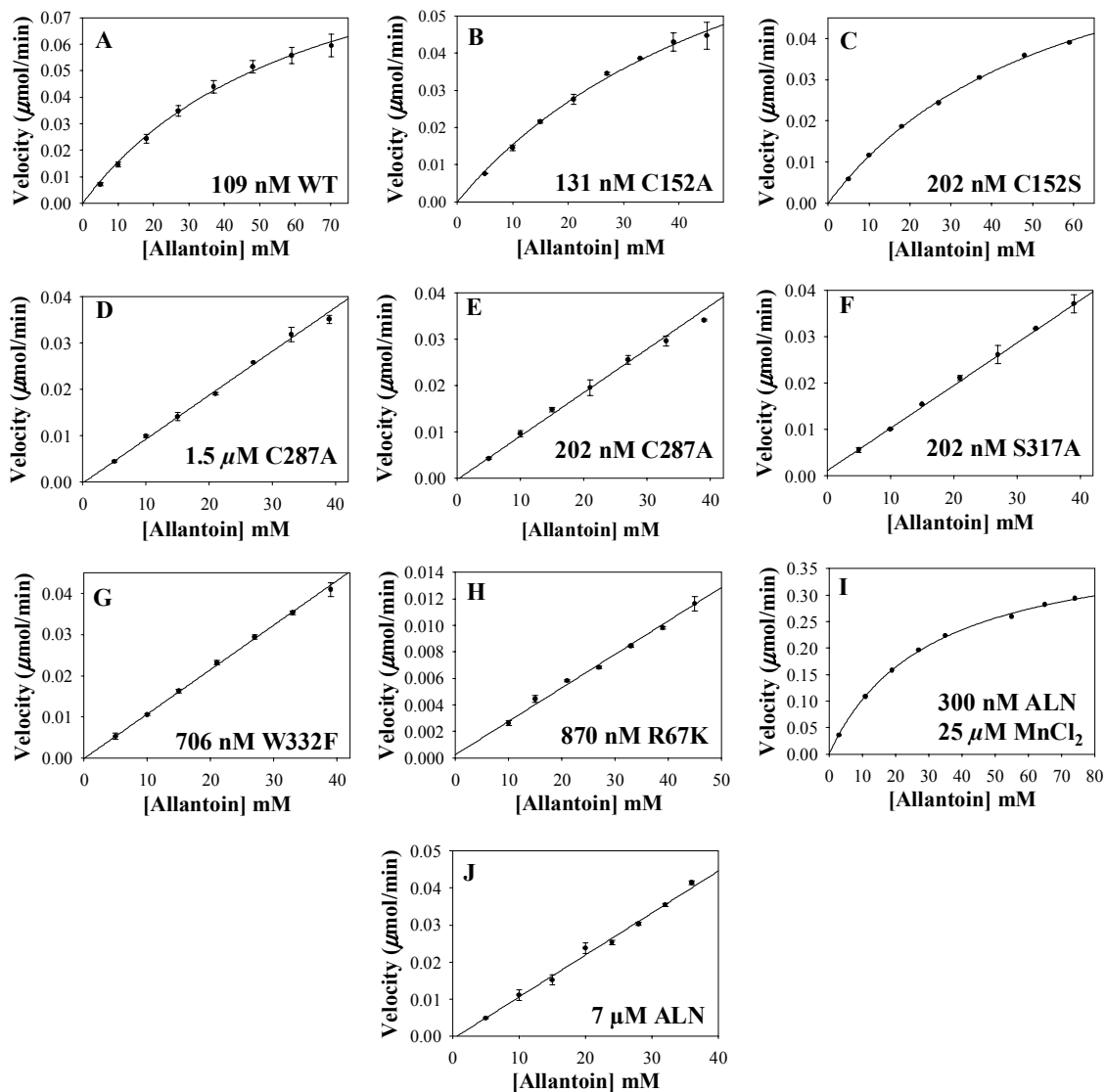


Figure 16: Substrate saturation plots for WT and mutant allantoinases. Velocity ($\mu\text{mol}/\text{min}$) vs. [allantoin] mM for plots for **A)** 109 nM WT, **B)** 202 nM C152S, **C)** 131 nM C152A, **D)** 1.5 μM C287A, **E)** 202 nM C287S, **F)** 202 nM S317A **G)** 706 nM W332F **H)** 870 nM R67K allantoinase at 20 °C and **I)** 300 nM low Zn content WT ALN sample A with Mn supplemented in assay 30 °C, pH 8.5 and **J)** same as I without MnCl_2 and 7 μM sample A enzyme. Plots A, B, C and I were fit to equation (1) and D, E, F, G, H and J fit to equation (2).

Table 12: Kinetic parameters for wild type and mutant allantoinases

Allantoinase Sample	k_{cat} , s^{-1}	K_M , mM	k_{cat}/K_M , $s^{-1}M^{-1}$
WT	19.4 ± 1.3	65 ± 7.6	298 ± 15
WT, MnCl ₂ in assay*	23 ± 0.4	30 ± 1.3	720 ± 34
WT, no MnCl ₂ in assay*	---	---	2.6 ± 0.05
R67K	---	---	4.7 ± 0.2
C152A	13.5 ± 1.1	59 ± 7.4	228 ± 10.4
C152S	6.5 ± 0.2	58 ± 3.3	111 ± 2.7
C287A	---	---	10.2 ± 0.3
C287S	---	---	72 ± 2.4
S317A	---	---	77 ± 0.9
W332F	---	---	25 ± 0.4

* Purified sample A allantoinase

DISCUSSION AND CONCLUSIONS

The goal of this research was to characterize the *E. coli* allantoinase. Metal ion dependence was studied using different divalent cations in the enzyme and determining the effects on the pK_1 . The pH rate profiles were compared to determine the roles of the ionizable protein side chains. A hypothetical structural model and amino acid sequence alignments were used to form a hypothesis as to which amino acids are important for catalysis. The catalytic and substrate binding roles of conserved amino acid residues were probed by site-directed mutagenesis.

In earlier experiments where allB was overexpressed in pBS+ in *E. coli*, the enzyme produced had low activity and little Zn content (sample A, B). In order to obtain improved overexpression of *allB*, *allB* was recloned from pBS+ into the pET30a+ vector. To produce ALN with high activity, overexpression occurred in TB media supplemented with high concentrations of Zn, Co, or Mn. The WT allantoinase was characterized in terms of its kinetic parameters, metal content, and pH-dependence with Zn, Co or Mn present.

From Michaelis-Menten plots of the velocity for the conversion of allantoin to allantoate as a function of allantoin concentration, k_{cat} , K_M , and k_{cat}/K_M were determined to be $19 \pm 1.3 \text{ s}^{-1}$, $65 \pm 8 \text{ mM}$ and $298 \pm 15 \text{ s}^{-1}\text{M}^{-1}$, respectively for ZnALN. Double reciprocal plots were used to determine k_{cat}/K_M for ALN in the presence of MnCl_2 , ZnALN and CoALN at pH 5-10. The pH rate profiles showed diminished activity at high and low pH. Specifically, pK_1 was 7.8, 5.3, and 5.7 for ALN in the presence of Mn, ZnALN and CoALN, respectively. The pK_2 values at high pH were all similar and

ranged from 8.7 to 8.9. The pK_1 was dependent on the divalent cation present. The ALN enzyme sample assayed in the presence of Mn was almost completely devoid of Zn and Mn. It is expected that the decrease in activity observed at high pH was due to ionization of allantoin. A pK_a of 9.1 ± 0.03 was assigned to the N3 hydrogen of allantoin as determined by ^{13}C NMR titration in D_2O (35).

For all purified WT and mutant forms of ALN, the metal content was determined. There is clearly a dependence on divalent cations for activity. Higher Zn content was associated with increased ZnALN activity. Manganese, Co and Ni all enhanced the allantoinase activity of sample A when present in the assay. Manganese provided the greatest enhancement with a k_{cat}/K_M of $720 \pm 34 \text{ s}^{-1}\text{M}^{-1}$ compared to $2.6 \pm 0.05 \text{ s}^{-1}\text{M}^{-1}$ for sample A ALN in the absence of added cation. However, the positive affect of Mn was less for enzyme samples with higher bound Zn or Mn content as purified. There was a ten-fold difference in the activity between sample A supplemented with Mn in the assay, 3.1 U/mg, and MnALN with 1 equivalent of bound Mn, 27 U/mg. The pK_1 in the presence of Mn compared to enzyme with bound Zn or Co was separated by ~ 2 pH units. This does not follow the trend for phosphotriesterase where the pK_a values with bound Zn, Co, and Mn are 5.8, 6.5, and 7.0, respectively (12). The Mn supplemented in the assay could be binding in the more solvent-exposed β position, polarizing the O4 oxygen of allantoin and partially stabilizing the tetrahedral intermediate. It may be that the activity would increase beyond pH 7.8 if not for the deprotonation of another group or the substrate. Allantoinase activity was highest when Co was bound to the enzyme. Zinc ALN, CoALN, and MnALN all contained between

1.4 and 2.2 equivalents of bound metal. This is further evidence that this enzyme ligates two metals. There is a general trend where less Zn content is observed as the protein yield and cell mass/L culture increases (Table 6). Even in the presence of 1.0 mM Co or 3.0 mM Mn in the *E. coli* culture during overexpression of *allB*, there was always Zn contamination, in the range of 5-90% of the equivalents of the desired cation, in the purified enzyme. According to the research conducted by Hausinger and coworkers, using Mn in the growth culture did not result the production of enzyme with enhanced activity over control (3); however, is not the case as seen in the results presented here. The MnALNa and MnALNb samples show a higher activity than ZnALN, and a higher Mn content was associated with increased MnALN activity. When *allB* was overexpressed without added metal in the *E. coli* culture, the highest activity obtained was 2 units/mg and contained 0.5 equivalents of Zn. Therefore, it is expected that Zn is the native metal for ALN.

It was clear that there was a large difference in enzyme characterization when metal was supplemented in the assay versus the same metal actually being bound in the enzyme. For example, supplementing sample A with Zn showed no increase in activity, but clearly ZnALN has activity and is less labile to dilution than CoALN or MnALN. There was also interest in performing electron paramagnetic resonance spectroscopy on MnALN to see a binuclear Mn signal. The easiest way to obtain ALN with bound Ni, Co, Mn and Cd would be to reconstitute the apoALN. If maximum activity were obtained at 2 equivalents of divalent cation, this would also be further proof that the enzyme was binuclear. Additionally, the requirement of bicarbonate for reconstitution

would be evidence for a carboxylated lysine. Dipicolinate was used to chelate Zn or Co from ZnALN and CoALN. The attempt to remove Zn was unsuccessful. However, all of the Co, as well as some of the Zn contamination, could be removed from CoALN. Treatment of the apo enzyme, obtained from CoALN, with bicarbonate and Zn or Mn did not result in increased activity. This problem was not alleviated by using degassed buffers and reducing agent during metal removal and reconstitution. It has been suggested by Hausinger that an accessory protein could be involved in the incorporation of metal in the active site as is the case for urease (13).

Since apoALN could not be reconstituted, MnALN had to be made in the same way as ZnALN and CoALN. The production of MnALN proved problematic due to high Zn contamination. By culturing *E. coli/AllBP-6* in the presence of 3 mM Mn by the standard protocol, a 1:1 ratio of Zn:Mn was obtained in the purified enzyme. Growth experiments were performed to determine if different conditions would allow for the production of MnALN with higher equivalents of Mn and less Zn contamination. At first it was thought that longer overexpression times were required after the addition of IPTG. It was determined that under standard growth conditions, maximal activity was obtained at varying incubation times following the addition of IPTG. The allantoinase activity of cell culture lysates needed to be monitored, and the cells harvested at the time of highest activity. The MnALN purified had an improved Zn:Mn ratio of ~ 1:3, but still only one equivalent of Mn and a considerably high contamination of Zn (0.35 equivalents). Fluctuation in specific activity of crude cell extracts during growth

experiments could have been due to instability of diluted enzyme either in the assay or during treatment with Bugbuster[®].

To choose amino acid residues to mutate based solely on sequence alignments is too broad of a starting point for site-directed mutagenesis. A three-dimensional structural model of *E. coli* ALN was constructed by aligning the ALN amino acid sequence onto the 2.6 Å resolution crystal structure of L-hydantoinase (26). This hypothetical ALN structure was then overlaid with DHO (12) in order to obtain a dihydroorotate in the active site. Dihydroorotate was then changed to allantoin, with atoms N1, C2, N3 and C4 of allantoin in the same position as dihydroorotate. Allantoin was in the S form in the model for two reasons—according to Hausinger, *et. al.* (3), the S-form was preferred and also experimental results mentioned here show that only one half of the substrate is consumed. Residues C152, S317, C287, S288, and W332 were considered to possibly contact the substrate. Serine 288 was not completely conserved. Aspartic acid 315 was expected to be the catalytic residue involved in acid/base catalysis. Arginine 67 is completely conserved and was predicted to be located in a loop region after the first β -strand of the $(\alpha\beta)_8$ barrel. Since H316 was completely conserved, it was also selected for mutagenesis. The following amino acid mutations were made by the method of QuickChange[®] mutagenesis: R67K, C152A, C152S, S317A, C287A, C287S, W332F, H316A, H316N, and D315N. Site-directed mutagenesis was used to determine the necessity of selected amino acids for catalysis and substrate binding based on the k_{cat} , K_{M} and $k_{\text{cat}}/K_{\text{M}}$.

Serine 317 was considered to possibly interact with the substrate because it is completely conserved among allantoinases, and the alcohol oxygen was in close proximity to the N8 hydrogens of allantoin in the model. The S317A mutant was used to test this hypothesis. Clearly, S317A was not essential for activity. Substrate binding was affected in that substrate saturation could not be reached. A hyperbolic relationship, between velocity and allantoin concentration, could be seen at higher substrate concentrations of 59 mM (not shown) but was insufficient to fit the data to equation 1. It is possible that S317 is not involved in a side-chain interaction, but is a backbone interaction instead.

Cysteine 287 was sensitive to the type of amino acid mutation. The C287S mutant had a 4-fold decrease in k_{cat}/K_M , but k_{cat}/K_M for C287A decreased 30-fold compared to WT. Cysteine 287 may be involved in a hydrogen-bonding interaction with the substrate. A strictly hydrophobic side chain in this position was not well tolerated. According to the model, C287A is equidistant from the carbonyl oxygen on C2 of allantoin, $\sim 5 \text{ \AA}$, and the D315 carboxyl at $\sim 6 \text{ \AA}$. Cysteine 287 is completely conserved among all allantoinases and hypothetical/putative allantoinases in the *E. coli* allantoinase amino acid sequence BLAST search. Mutations C152S and C152A had diminished k_{cat}/K_M , but similar K_M to WT, and were considerably more tolerated than any of the other mutations.

The metal-liganding Asp residue, common to many binuclear amidohydrolase superfamily members, was predicted to be D315 based on sequence alignments with other amidohydrolase enzymes and the strict conservation of this residue among

allantoinases. Even though D315 was predicted to be a metal ligand, the purified D315N mutant contained a similar amount of Zn to the rest of the mutant and WT ALNs. This was very fortuitous because the absence of enzymatic activity for the D315N mutant could not be attributed to the absence of Zn. It is concluded that D315 is catalytically essential residue which acts as an acid/base in the catalytic mechanism of hydrolysis. These results do not disprove that D315 binds the α Zn because there are other ligands which are expected to contribute to the complexation of Zn, namely H59, H61, and carboxylated K146. For example, the D301N mutant of phosphotriesterase is able to bind Zn and has a small amount of activity (14).

Arginine 67 was chosen for mutagenesis because it was a conserved charged amino acid. Arginine 67 is predicted to be in the loop region after the first β -strand and may interact with the substrate if its position were to shift with loop movement. The drastic reduction on catalytic efficiency, $4.7 \text{ s}^{-1}\text{M}^{-1}$ compared to $300 \text{ s}^{-1}\text{M}^{-1}$ for WT, was unexpected. The nearest interaction to R67 is D160 at $\sim 2\text{\AA}$ in the model. In the allantoinase sequence alignment, D160 is semiconserved in that the only other amino acid in this position is glutamate. This is an interaction on the exterior of the enzyme in the model. The delocalized positive charge of arginine can interact with a carboxyl group, but the substrate would have to be oriented differently for this residue to stabilize the carboxylate that is formed in the product, allantoate. A couple of other reasonable interactions with the ureide motif of allantoin are shown in Figure 17 and are based on the orientation of electrophilic and nucleophilic atoms in the two molecules. The ureide substituent off of C5 is likely to be important for substrate binding; according to the

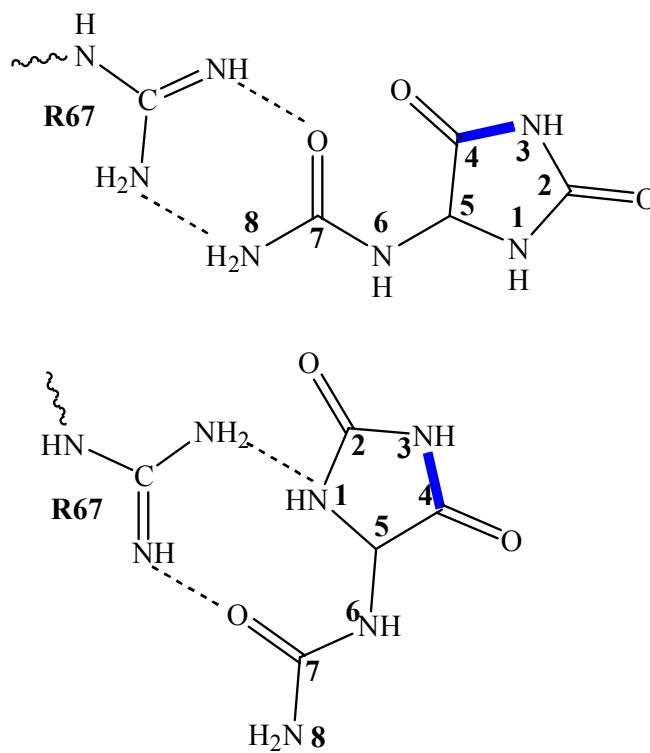
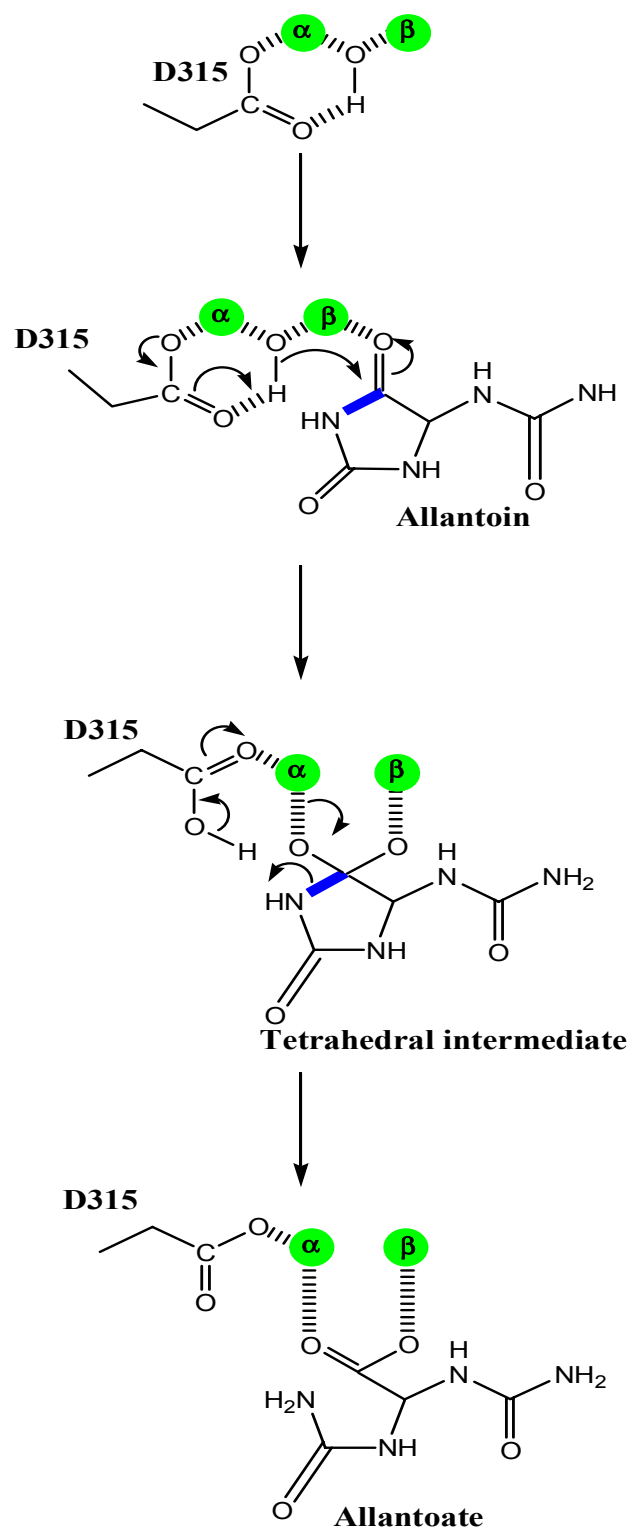


Figure 17: Possible interactions between allantoin and R67 of allantoinase. The bond cleaved by allantoinase is highlighted in blue.

literature, allantoinase hydrolyzes the same cyclic amide bond of hydantoin and isopropylhydantoin with 2% and 0.3% the specific activity for allantoin, respectively (20).

A mutation to phenylalanine is the most conservative mutation which can be made for tryptophan, yet the $k_{\text{cat}}/K_{\text{M}}$ for W332F decreased by an order of magnitude to $25 \text{ s}^{-1}\text{M}^{-1}$. If tryptophan were in contact with the substrate, the N1 nitrogen of W332 could be hydrogen bonding to NH hydrogens of allantoin. Tryptophan 332 may be providing a steric affect. Figure 15, shown previously, presents a view of the orientation of the mutated residues with respect to each other and allantoin in the structural model. The current proposed mechanism is depicted in Scheme 4 and is based on previous work (12, 14, 21). The enzyme has two Zn ions which function to activate a water molecule to a hydroxide. The hydroxide is positioned between D315 and the more buried α Zn ion and attacks carbon 4 of allantoin to yield a tetrahedral intermediate which is stabilized by the two Zn ions. The amide bond is then cleaved with the formation of the carboxylate group and acceptance of a proton by N1 of allantoin from D315.

Scheme 4: Proposed mechanism of allantoinase

REFERENCES

1. Drift, C. van der, (1976) Degradation of purines and pyrimidines, *Bacteriol. Rev.* 40, 404-429.
2. Vogels, G.D., Trijbels, F., and Uffink, A. (1966) Allantoinases from bacterial, plant and animal sources, *Biochim. Biophys. Acta* 122, 482-496.
3. Mulrooney, S.B., and Hausinger, R.P. (2003) Metal ion dependence of recombinant *Escherichia coli* allantoinase, *J. Bacteriol.* 185, 126-134.
4. Yang, J., and Han, K.H. (2004) Functional characterization of allantoinase genes from *Arabidopsis* and a nonureide-type legume black locust, *Plant Physiol* 134, 1039-1049.
5. Piedras, P., Aguilar, M., and Pineda, M. (1998) Uptake and metabolism of allantoin and allantoate by cells of *Chlamydomonas reinhardtii*, *Eur. J. Phycol.* 33, 57-64.
6. Hayashi, S., Jain, S., Chu, R., Alvares, K., Xu, B., Erfurth, F., Usuda, N., Sambasiva, M., Reddy, S.K., Noguchi, T., Reddy, J.K., and Yeldandi, V. (1994) Amphibian allantoinase: Molecular cloning, tissue distribution and functional expression, *J. Biol. Chem.* 269, 12269-12276.
7. Gaines, P.J., Brandt, K.S., Eisele, A.M., Wagner, W.P., Bozic, C.M., and Wisnewski, N. (2002) Analysis of expressed sequence tags from subtracted and unsubtracted *Ctenocephalides felis* hindgut and malpighian tubule cDNA libraries, *Insect Mol. Biol.* 11, 299-306.
8. Webb, M.A., and Lindell, J.S. (1993) Purification of allantoinase from soybean seeds and production and characterization of anti-allantoinase antibodies, *Plant Physiol.* 103, 1235-1241.
9. Cusa, E., Obradors, N., Baldoma, L., Badia, J., and Agular, J. (1999) Genetic analysis of a chromosomal region containing genes required for assimilation of allantoin nitrogen and linked glyoxylate metabolism in *Escherichia coli*, *J. Bacteriol.* 181, 7479-7484.
10. Schultz, A.C., Nygaard, P., and Saxild, H.H. (2001) Functional analysis of 14 genes that constitute the purine catabolic pathway in *Bacillus subtilis* and evidence for a novel regulon controlled by the PucR transcription activator, *J. Bacteriol.* 183, 3293-3302.
11. Ireton, G.C. McDermott, G., Black, M.E., and Stoddard, B.L. (2002) The structure of *Escherichia coli* cytosine deaminase, *J. Mol. Biol.* 315, 687-697.

12. Thoden, J.B., Phillips, G.N., Neal, T.M., Raushel, F.M., and Holden, H.H. (2001) Molecular structure of dihydroorotase: A paradigm for catalysis through the use of a binuclear metal center, *Biochemistry* 40, 6989-6997.
13. Jabri, E., Carr, M.B., Hausinger, R.P., and Karplus, A. (1995) The crystal structure of urease from *Klebsiella aerogenes*, *Science* 268, 998-1004.
14. Aubert, S.D., Li, Y., and Raushel, F.M. (2004) Mechanism for the hydrolysis of organophosphates by the bacterial phosphotriesterase, *Biochemistry* 43, 5707-5715.
15. Benning, M.M., Shim, H., Raushel, F.M., and Holden, H.M. (2001) High resolution X-ray structures of different metal-substituted forms of phosphotriesterase from *Pseudomonas diminuta*, *Biochemistry* 40, 2712-2722.
16. Liaw, S.H., Chem, S.J., Ko, T.P., Hsu, C.S., Chen, C.J., Wang, A., and Tsai, Y.C. (2003) Crystal structure of D-aminoacylase from *Alcaligenes faecalis* DA1, *J. Biol. Chem.* 278, 4957-4962.
17. Omburo, G.A., Kuo, J.M., Mullins, L.S., and Raushel, F.M. (1992) Characterization of the zinc binding site of bacterial phosphotriesterase, *J. Biol. Chem.* 267, 13278-13283.
18. Huang, D.T.C., Thomas, M.A.W., and Christopherson, R.I. (1999) Divalent metal derivatives of the hamster dihydroorotase domain, *Biochemistry* 38, 9964-9970.
19. Porter, D.J.T., and Austin, E.A. (1993) Cytosine deaminase: The roles of divalent metal ions in catalysis, *J. Biol. Chem.* 268, 24005-24011.
20. Kim, G.J., Lee, D.E., and Kim, H.S. (2000) Functional expression and characterization of the two cyclic amidohydrolase enzymes, allantoinase and a novel phenylhydantoinase, from *Escherichia coli*, *J. Bacteriol.* 182, 7021-7028.
21. Thoden, J.B., Marti-Arbona, R., Raushel, F.M., and Holden, H.H. (2003) High-resolution X-ray structure of isoaspartyl dipeptidase from *Escherichia coli*, *Biochemistry* 42, 4874-4882.
22. Wise, E.L., and Rayment, I. (2004) Understanding the importance of protein structure to nature's routes for divergent evolution in TIM barrel enzymes, *Acc. Chem. Res.* 37, 149-158.
23. Masuda, W., Fujiwara, S., and Noguchi, T. (2001) A new type of allantoinase in amphibian liver, *Biosci. Biotechnol. Biochem.* 65, 2558-2560.

24. Noguchi, T., Fujiwara, S., and Hayashi, S. (1986) Evolution of allantoinase
allantoicase involved in urate degradation in liver peroxisomes, *J. Biol. Chem.* *261*,
4221-4223.
25. Abendroth, J., Niefind, K., and Schomburg, D. (2002) X-ray structure of
dihydropyrimidinase from *Thermus* sp. At 1.3 Å resolution, *J. Mol. Biol.* *320*,
143-156.
26. Abendroth, J., Niefind, K., May, O., Siemann, M., Sydatk, C., and Schomburg, D.
(2002) The structure of L-hydantoinase from *Arthobacter aurescens* leads to an
understanding of dihydropyrimidinase substrate and enantio specificity,
Biochemistry *41*, 8589-8597.
27. Xu, Z., Liu, Y., Yang, Y., Jiang, W., Arnold, E., and Ding, J. (2003) Crystal structure
of D-hydantoinase from *Burkholderia pickettii* at a resolution of 2.7 angstroms:
Insight into the molecular basis of enzyme thermostability, *J. Bacteriol.* *185*,
4038-4049.
28. Gilmore, J.A., Liu, J., Gao, D.Y., and Critser, J.K. (1997) Determination of optimal
cryoprotectants and procedures for their addition and removal from human
spermatozoa, *Human Reproduction* *12*, 112-118.
29. Chazan, A. (2002 January) Peptide property calculator. Evanston, IL: Northwestern
University: <http://www.basic.nwu.edu/biotool/ProteinCalc.html>.
30. Pace, C.N., Vajdos, F., Fee, L., Grimsley, G., and Gray, T. (1995) How to measure
and predict the molar absorption coefficient of a protein, *Protein Sci.* *4*, 2411-2423.
31. Bradford, M. (1976) A rapid and sensitive method for the quantitation of microgram
quantities of protein utilizing the principle of protein-dye binding, *Anal. Biochem.*
72, 248-254.
32. Romanov, V., Merski, M.T., and Hausinger, R.P. (1999) Assays for allantoinase,
Anal. Biochem. *268*, 49-53.
33. Datsenko, K.A., and Wanner, B.L. (2000) One-step inactivation of chromosomal
genes in *Escherichia coli* K-12 using PCR products, *PNAS* *97*, 6640-6645.
34. Studier, F.W., and Moffatt, B.A. (1986) Use of bacteriophage T7 RNA polymerase
to direct selective high-level expression of cloned genes, *J. Mol. Biol.* *189*, 113-130.
35. Kahn, K., Serfozo, P., and Tipton, P.A. (1997) Identification of the true product of
the urate oxidase reaction, *J. Am. Chem. Soc.* *119*, 5435-5442.

VITA

Jennifer Ann Cummings

PERMANENT ADDRESS

1593 Roberts Road
Medford, OR 97504
(541) 779-7492

EDUCATION**M.S. Chemistry**

Texas A&M University, College Station, TX, May 2005

B.S. Chemistry/Biochemistry

Southern Oregon University, Ashland, OR, June 2001